

See discussions, stats, and author profiles for this publication at: <https://www.researchgate.net/publication/233825221>

Radiometals for Combined Imaging and Therapy

ARTICLE *in* CHEMICAL REVIEWS · NOVEMBER 2012

Impact Factor: 46.57 · DOI: 10.1021/cr3003104 · Source: PubMed

CITATIONS

86

READS

33

5 AUTHORS, INCLUDING:



[Cathy Sue Cutler](#)

Brookhaven National Laboratory

82 PUBLICATIONS 1,600 CITATIONS

[SEE PROFILE](#)



[Sandrine Hulier](#)

University of Nantes

50 PUBLICATIONS 380 CITATIONS

[SEE PROFILE](#)



[Silvia Jurisson](#)

University of Missouri

137 PUBLICATIONS 3,135 CITATIONS

[SEE PROFILE](#)

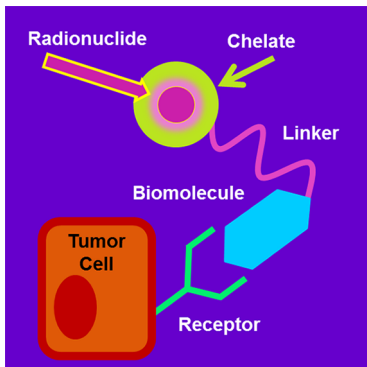
Radiometals for Combined Imaging and Therapy

Cathy S. Cutler,^{*,†} Heather M. Hennkens,[†] Nebiat Sisay,^{†,‡} Sandrine Huclier-Markai,[§] and Silvia S. Jurisson[‡]

[†]University of Missouri Research Reactor Center, Columbia, Missouri 65211, United States

[‡]Department of Chemistry, University of Missouri, Columbia, Missouri 65211, United States

[§]Laboratoire Subatech, UMR 6457, Ecole des Mines de Nantes/Université de Nantes/CNRS-IN2P3, 4 Rue A. Kastler, BP 20722, F-44307 Nantes Cedex 3, France



CONTENTS

1. Introduction	858
2. Diagnostic Imaging	859
2.1. Gamma Emitters	859
2.2. Positron Emitters	859
3. Therapeutic Requirements	860
4. Theranostics	862
5. Radionuclides for Imaging and Therapy	862
5.1. Gold-198	862
5.2. Gold-199	864
5.3. Rhodium-105	864
5.4. Lanthanides	865
5.4.1. Lutetium-177	866
5.4.2. Samarium-153	869
5.4.3. Holmium-166	869
5.4.4. Terbium-161	870
5.4.5. Promethium-149	870
5.5. Rhenium-186 and -188	870
5.6. Scandium-44 and -47	871
5.7. Copper-64 and -67	873
5.8. Arsenic-71, -72, -74, and -77	875
5.9. Lead-212	875
5.10. Bismuth-212 and -213	876
5.11. Tin-117m	877
5.12. Gallium-67 and Indium-111	877
6. Summary	878
Author Information	878
Notes	878
Biographies	878
References	879

1. INTRODUCTION

The use of radionuclides in medicine is based largely on the discoveries of two critical concepts, the “tracer principle” and the “magic bullet”. In 1913, George de Hevesy developed the tracer approach and was the first to recognize that radionuclides could be used as tracers to follow how the native element or compound containing the element was distributed either in plants or in animals.¹ He based his theory on the principle that radioactivity has the advantage of being easily detected at very low quantities, allowing for the introduction of minute quantities, nano- to picomoles, that will not perturb the system. Thus the radiolabeled tracer allows for noninvasive measurement of distribution and function in a biological system. Paul Ehrlich later developed the “magic bullet” concept highlighting how biomolecules, particularly antibodies, could be utilized as targeting molecules to transport toxins selectively to cancerous tissues. For example, radionuclides can be attached to antibodies that are selective for receptors that are overexpressed on a certain disease site such as tumor cells. This concept has been expanded to include a host of nanocarriers, from small molecules such as folic acid to peptides and proteins, microspheres, and most recently nanoparticles. Both concepts have been utilized to develop radiopharmaceuticals.

Radiopharmaceuticals are drugs that consist of two parts: a radionuclide that imparts the mechanism of action through its decay and a targeting biomolecule or organic ligand that determines the localization of the radiopharmaceutical. They can be used either as diagnostics for the noninvasive imaging of disease or as therapeutics to deliver a toxic payload selectively, for instance, to a tumor site. Most of the development and optimization of radiopharmaceuticals occurs when designing or modifying the target selectivity of the molecule, not the mechanism of action, as with other drugs. Diagnostic agents consist of radionuclides that decay to release photons with a high enough energy to penetrate the body and be detected externally but low enough to be collimated by a camera. Therapeutic agents consist of radionuclides that decay to release a particle, such as a β^- or α particle that can cause ionization and break bonds resulting in the intended ablation. Until recently most radiopharmaceuticals were designed to be used solely for either diagnostics or therapeutics. It was thought

Special Issue: 2013 Nuclear Chemistry

Received: August 1, 2012

Published: November 30, 2012

that imaging required a radionuclide that decays solely by photon emission with energy suitable for imaging and that any release of particles would give an undesired additional dose to the patient. The initial thinking in the case of therapeutics was similar, that little was gained but dose to both the patient and medical personnel when administering radionuclides that emitted not only the desired particles for treatment but also photons.

As the development of drugs that target specific pathways advanced, the use of the same targeting biomolecule or organic ligand for both imaging and therapy began but with attachment to two different radionuclides. One radionuclide would be used to image individual patient disease states and evaluate their receptor expression, metabolic rate, clearance, and handling, and a second radionuclide would be used for therapy. Problems with this approach arose due to differences in the chemistry of the radionuclides themselves, which have been shown to affect the overall distribution and mechanism of localization, resulting in an over- or underestimation of dose to critical tissues and the dose being outside the optimum range of efficacy. Agents currently being designed utilize radionuclides that give off photons that can be imaged as well as particles that can be used for treatment. Besides the obvious advantages of more exact patient assessment and dosage, there are significant savings of time and other resources when developing one drug that can serve two purposes rather than two separate drugs. A new term has been coined for these drugs: "theranostics". This review presents radiometals that have the nuclear properties required for use in theranostic applications for imaging and therapy. Their chemistry and production methods are discussed, along with examples of preclinical and clinical uses. The intention of the review is not to cover every possible radiometal that can be used or to include all applications of presented radiometals but to give the reader a basic comprehension of what radiometals have been most commonly used and how their nuclear properties and chemistries dictate their use in applications.

2. DIAGNOSTIC IMAGING

2.1. Gamma Emitters

Radionuclide imaging is divided into two modalities based on the type of decay and resultant emission and detection. Single photon emission computed tomography (SPECT) is the most prevalent and is based on radionuclides that emit photons between 70 and 360 keV.² Diagnostic imaging requires radiation that can penetrate the body and be detected by instrumentation that is external to the patient, and this necessitates radionuclides that emit photons such as γ rays (γ) or annihilation photons from positrons (β^+) without accompanying alpha (α) or beta (β^-) particle emissions. The energy needs to be higher than 50 keV to escape the body but low enough to be collimated easily. Recent advances in SPECT cameras, such as the type of collimators, detectors, and image reconstruction methods, are raising the upper energy limit and allowing the detection of two or more photon energies or radionuclides at the same time. This permits detection of a variety of biomarkers in one image, enhancing our ability to individualize patient diagnosis and subsequent treatment regimens. While positron emission tomography (PET) imaging provides better attenuation and scatter correction and superior quantification capabilities, the use of phantoms with SPECT along with some of the newer software designed for scatter and attenuation corrections has been shown to provide very

acceptable quantitative SPECT images. A number of radionuclides decay with γ emissions that are suitable for imaging, such as gallium-67 (^{67}Ga), iodine-123 (^{123}I), indium-111 (^{111}In), technetium-99m ($^{99\text{m}}\text{Tc}$), and thallium-201 (^{201}Tl).

Technetium-99m has been the most prevalently used radionuclide for diagnostics based on its favorable nuclear properties, including a single 140 keV photon emission (ideal for most γ cameras), absence of particle emission, a short half-life of 6.03 h, and availability via portable $^{99}\text{Mo}/^{99\text{m}}\text{Tc}$ generators. Technetium has a rich chemistry that has allowed for its incorporation into a plethora of formulations for a variety of drugs and according to the International Atomic Energy Association (IAEA) and World Nuclear Association is currently used in over 80% of nuclear diagnostic procedures. The use of $^{99\text{m}}\text{Tc}$ was further promoted by the development of kits, often called shake and shoot preparations, that allow for consistent quality preparations at multiple sites. Until fairly recently, $^{99\text{m}}\text{Tc}$ had the additional advantage of being readily available at a minimal cost. Recent problems encountered at aging reactor facilities have caused worldwide shortages and a scramble not only for new supply chains but also alternative radionuclides to meet current and projected demands. Table 1 lists some radionuclides of interest along with their nuclear properties.

2.2. Positron Emitters

PET is the second most common noninvasive imaging modality and is based on radionuclides that decay predominantly by emitting a positron that subsequently annihilates with an electron to produce two coincident 511 keV photons approximately 180° apart. A ring of detectors placed around the patient is used to detect the two coincident 511 keV photons, and electronic collimation, rather than lead collimation used in SPECT, is used to remove scatter and background. This allows for a lower amount of radioactivity to be used and for higher resolution and sensitivity than SPECT. Additionally, PET imaging allows for quantitative mapping of a drug or biomarker *in vivo*, which can be extremely important in evaluating whether a certain therapeutic can be utilized to target a receptor. The ideal nuclear properties for a PET radionuclide are low positron energy similar to that of fluorine-18 (^{18}F) with a maximum positron energy of 633.5 keV, which allows for optimal resolution, a high positron branching ratio, and a half-life that both matches that of the biomarker being labeled and allows for chemical synthesis and delivery of the agent to the clinic. Most positron emitters have very short half-lives, and the common radionuclides used for PET are nonmetals such as carbon-11 (^{11}C), oxygen-15 (^{15}O), nitrogen-13 (^{13}N), and fluorine-18 (^{18}F). These are common elements that make up biological molecules and thus can be incorporated without disturbing the overall behavior of the molecule. This tends not to be the case for most radiometals, which are large and, as is the case with Tc, are not commonly present in most biological molecules. The most prevalently used PET radionuclide is ^{18}F ; it can be made in rather large quantities and with modern automated remote boxes can be easily incorporated into a variety of biomolecules. The most common ^{18}F agent is ^{18}F -fluorodeoxyglucose, which is used for imaging high metabolic disorders such as inflammation and cancer.

Although the standard PET radionuclides have seen wide use, they suffer from having very short half-lives that lessen their use in some molecules and complicated time-consuming organic syntheses that are not always compatible with biomolecules. Recently, however, prosthetic groups have been

Table 1. Half-Life and Emission Properties of Medical Radioisotopes

radionuclide	type	$T_{1/2}$	$E_{\max} \beta, \text{MeV}$ (%)	γ energy, keV (%)
¹⁹⁸ Au	β^- , γ	2.694 d	0.96	412 (95.6)
¹⁹⁹ Au	β^- , γ	3.139 d	0.4526	208 (9.1) 158 (40)
¹⁰⁵ Rh	β^- , γ	35.36 h	0.566 0.248	319 (19.6) 306 (5)
¹⁷⁷ Lu	β^- , γ	6.64 d	0.498	208 (11) 113 (6.6)
¹⁵³ Sm	β^- , γ	46.27 h	0.808	103 (28.3)
¹⁶⁶ Ho	β^- , γ	26.83 h	1.8545	80.6 (6.2) 1379 (1.13)
¹⁶¹ Tb	β^- , γ	6.91 d	0.59	48.9 (17.0) 74.6 (10.2)
¹⁴⁹ Pm	β^- , γ	2.212 d	1.07	286 (3)
¹⁸⁶ Re	β^- , γ	3.72 d	1.07	137 (9)
¹⁸⁸ Re	β^- , γ	16.98 h	2.12	155 (15)
⁴⁴ Sc	β^+ , γ	3.97 h	0.632	511, 1157
⁴⁷ Sc	β^- , γ	3.345 d	0.600	159.4 (68)
⁶⁴ Cu	β^+ , β^- , γ (EC)	12.7 h	0.653 (19) 0.579 (40)	511 (38.6)
⁶⁷ Cu	β^- , γ	2.58 d	0.577	184.6 (46.7) 93.3 (16.6) 91.3 (7.3)
⁷¹ As	β^+ , γ	2.72 d	0.81	175 (82)
⁷² As	β^+ , γ	26.0 h	3.34	834 (80)
⁷⁴ As	β^+ , β^- , γ	17.8 d	1.36 (29) 1.54 (32)	596 (59.3)
⁷⁷ As	β^- , γ	38.8 h	0.68	239 (1.6)
²¹² Pb	β^- , γ	10.64 h	0.5737	238.6 (43.1)
²¹² Bi	α , β^-	60.55 min	2.25 (55.5)	727 (11.8)
²¹³ Bi	α , β^-	45.6 min	1.426 (97.9)	440 (27.3)
²²⁵ Ac	α	10 d	5.935	99 (5.8)
^{117m} Sn	IT	13.6 d	0.13–0.16	156 (2.1) 158.6 (86.3)
⁶⁷ Ga	EC	3.26 d		393.5 (4.2) 300 (15.3) 184.6 (20.8) 93 (38.6)
¹¹¹ In	EC	2.8 d		173 (89) 247 (95)

developed that allow for rapid attachment of ¹⁸F to proteins and antibodies. This limitation has led to the use of radiometals that decay by positron emission with longer half-lives allowing for use with the larger proteins and peptides, which have longer biological half-lives. A number of radiometals have been evaluated for PET due to their favorable nuclear properties and are listed in Table 1, and in Table 2 are listed their calculated mean tissue range, theoretical specific activity, and achieved specific activity.

3. THERAPEUTIC REQUIREMENTS

Radiotherapy involves the administration of a radioactive drug that is selectively accumulated in cancerous or diseased tissue versus normal tissue and either ablates or damages the diseased tissue through the emission of an energetic particle. This particle emission can be a β^- particle, a α particle, or an Auger electron (e^-). Because these particle emissions result in damage to tissue, it is imperative that the drug accumulates selectively in

the diseased tissue, because any uptake in normal tissue will result in unwanted dose to the patient and injury to normal tissue.

Several factors must be considered in choosing a particular radioisotope for therapeutic applications, such as physical half-life, energy of the particle emission, type of particle emission, specific activity, and the cost and availability of the radioisotope. The half-life must match the pharmacokinetics of the radioactive drug, specifically for uptake and clearance from normal versus targeted tissues, in order to maximize the dose to the target and minimize dose to normal tissue.

In choosing a therapeutic isotope for monoclonal antibodies, it is important to consider that it normally takes at least 4 days for monoclonal antibodies to clear the bloodstream and reach maximum uptake at the target site.³ Labeling monoclonal antibodies with an isotope with too short of a half-life will result in most of the dose being administered in normal tissues, with little to none reaching the target site. On the other hand, faster clearing small molecules and peptides can be labeled with short-lived isotopes and achieve maximum dose delivery in the target tissue. Half-life also affects how easily the isotope can be transported from the site of production to the final user. Short-lived isotopes require either on-site production, which can be prohibitively expensive, or development of a generator system.

Specific activity, a measure of the radioactivity per unit mass of the compound, is an indicator of potency; the higher the specific activity of a radionuclide, the higher both the percentage of radioactive atoms and the deliverable dose. Specific activity may or may not be important depending on the number of sites available for targeting. For instance, bone is considered a large capacity site and does not require radioisotopes with high specific activity. Low specific activity radioisotopes such as ¹⁵³Sm in Quadramet and ¹⁶⁶Ho in the skeletal targeted radiotherapy agent, STR, have been used for pain palliation and bone marrow ablation, respectively.⁴ Low capacity sites such as receptor sites, which are present in low numbers, require high specific activity radioisotopes.

The choice of type and energy of the particle emission is largely determined by the size of the lesion or tumor being treated, site of delivery, whether the tumor is homogeneous, and whether the dose can be delivered uniformly to each cell. For example, smaller tumors may respond better to lower β^- energies, such as for ¹⁷⁷Lu, whereas the higher energy β^- emitter ¹⁶⁶Ho may be required for larger tumors. In certain cases, the elimination or minimization of toxic side effects determines which energy is optimal.

The radiation doses required for tumor cell killing are highly dependent on the specific cancer to be treated (e.g., its radiation sensitivity), type of particle emission (α particles, β^- particles, and Auger electrons), the radionuclide particle energy (especially for β^- particles or high energy electrons), the tumor size and location, and the nontarget radiation dose delivered by the radiopharmaceutical. α -Particles are high linear energy transfer (LET) radiation and produce very high localized ionization densities in cells that minimize the ability of the cells to repair radiation damage. α -Particles are therefore most effective in cell killing (per gray delivered); however, their range is short (approximately one to three cell diameters) and best suited for small tumors; α -particles deposited in tumors deliver minimal irradiation of nearby tissues. Auger emitters produce very low energy electrons that have very short ranges and are considered a form of high LET radiation. Because of their subcellular ranges, the Auger-emitting radionuclides must be

Table 2. Radiometal Nuclear Properties, Theoretical and Achievable Specific Activities, and Calculated Mean Tissue Ranges

radionuclide	decay mode	$T_{1/2}$ (h)	$E_{\max} \beta^-$, MeV (%)	γ energy, keV (%)	theoretical specific activity		achievable specific activity Ci/mg	ref ^a	mean tissue range ^b (mm)
					Ci/ μmol	Ci/mg			
¹⁹⁸ Au	β^- , γ	64.7	0.96	412 (95.6)	4.8	245	0.095	1	0.38
¹⁹⁹ Au	β^- , γ	75.4	0.45	208 (9.1) 158 (40)	4.1	210			0.14
¹⁰⁵ Rh	β^- , γ	35.4	0.57 0.25	319 (19.6) 306 (5)	8.8	843			0.19
¹⁷⁷ Lu	β^- , γ	161.0	0.50	208 (11) 113 (6.6)	1.9	110	25	1	0.16
¹⁵³ Sm	β^- , γ	46.3	0.81	103 (28.3)	6.7	443	6	1	0.30
¹⁶⁶ Ho	β^- , γ	26.8	1.86	80.6 (6.2) 1379 (1.13)	11.6	704	22	1	0.84
¹⁶¹ Tb	β^- , γ	165.8	0.59	48.9 (17.0) 74.6 (10.2)	1.9	117			0.20
¹⁴⁹ Pm	β^- , γ	53.1	1.10	286 (3)	5.9	396			0.43
¹⁸⁶ Re	β^- , γ	89.2	1.10	137 (9)	3.5	189	3	1	0.43
¹⁸⁸ Re	β^- , γ	16.9	2.10	155 (15)	18.4	984	c	2	0.98
⁴⁴ Sc	β^+ , γ	3.9	0.63	511(94) 1157 (99.9)	79.5	181			
⁴⁷ Sc	β , γ	80.4	0.60	159.4 (68)	3.9	830			0.20
⁶⁴ Cu	β^+ , β^- , γ (EC)	12.7	0.65 (19) 0.58 (40)	511 (38.6)	24.6	3,855			0.19
⁶⁷ Cu	β^- , γ	61.9	0.58	184.6 (46.7) 93.3 (16.6) 91.3 (7.3)	5.0	755			0.19
⁷¹ As	β^+ , γ	65.3	0.81	175 (82)	4.8	676			
⁷² As	β^+ , γ	26.0	3.34	834 (80)	12.0	1674			
⁷⁴ As	β^+ , β^- , γ	426.7	1.36 (29) 1.54 (32)	596 (59.3)	0.7	99			0.58
⁷⁷ As	β^- , γ	38.8	0.68	239 (1.6)	8.0	1048			0.24
²¹² Pb	β^- , γ	10.6	0.57	238.6 (43.1)	29.3	1389			0.19
²¹² Bi	α , β^-	1.0	2.25 (55.5)	727 (11.8)	309.4	1465			
²¹³ Bi	α , β^-	0.8	1.43 (97.9)	440 (27.3)	410.1	19324			
²²⁵ Ac	α	240.0	5.94	99 (5.8)	1.3	58			
^{117m} Sn	IT	326.4	0.13–0.16	156 (2.1) 158.6 (86.3)	1.0	82	0.008–0.010	3	
⁶⁷ Ga	EC	78.3		393.5 (4.2) 300 (15.3) 184.6 (20.8) 93 (38.6)	4.0	598	1.0	4	
¹¹¹ In	EC	67.3		173 (89) 247 (95)	4.6	49	c	5	

^aThe achievable specific activity values were obtained from the following, as referenced: (1) Radioisotopes and radiochemicals. http://www.murri.missouri.edu/ps_radio_isotopes.php (accessed October 1, 2012). (2) Knapp, J., Nuclear medicine program progress report, Oak Ridge National Lab, 1996. (3) Knap, J., Production of Medical radioisotopes in the ORNL high flux isotope reactor (HFIR). 13th Radiochemical conference, Marainske Lazne, Czech Republic, 1999, in press. (4) Ga-67 Fact Sheet. http://www.nordion.com/documents/products/Ga-67_Can.pdf (accessed October 1, 2012). (5) PerkinElmer. <http://www.perkinelmer.com/catalog/category/id/radiochemicals> (accessed October 1, 2012). ^bThe values for the estimated mean tissue range were calculated by following the standard formula referenced in Loveland, W. D.; Morrissey, D. J.; Seaborg, G. T. *Modern Nuclear Chemistry*; John Wiley & Sons: Hoboken, NJ, 2005. ^cNo carrier added.

deposited within or extremely close to the nucleus of the cell for maximum effectiveness. β -Particles are low LET radiation and generally have ranges in soft tissue of a few micrometers to a few centimeters. Thus, low to medium energy β^- particle-emitting radionuclides (e.g., ¹⁷⁷Lu) are considered more effective for treating small tumors, while high energy β^- particle-emitting radionuclides (e.g., ⁹⁰Y) are more appropriate for treatment of larger tumors. In all cases, the radiation dose delivered to nontarget tissues and organs (namely, the

maximum tolerable radiation dose) will be a critical factor in determining the maximum activity (MBq/mCi) that can be administered to the patient. For more details on this subject, the reader is directed to the ref 5.

Finally, the cost and availability of the radionuclide ultimately determines whether it is used. Generators are ideal for radionuclide production because they provide the radionuclide as needed at a relatively low cost, and most have a long shelf life. Few therapeutic radionuclides are available in generator

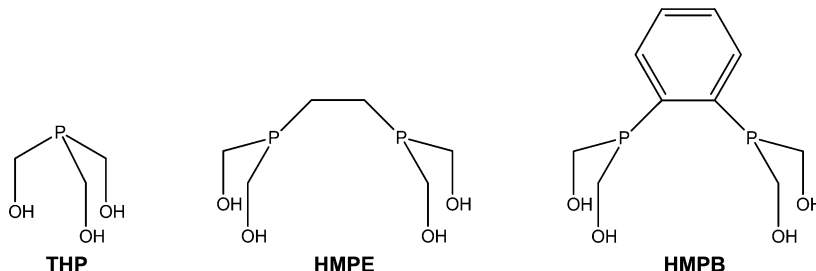


Figure 1. Structures of gold phosphine ligands (THP, HMPE, and HMPB).

form. The most notable generator of a therapeutic radionuclide is the $^{188}\text{W}/^{188}\text{Re}$ generator currently provided by the high flux reactor ($2 \times 10^{15} \text{ N cm}^{-2} \text{ s}^{-1}$) at Oak Ridge National Laboratory and others. Besides generator production, therapeutic isotopes can be produced most economically at medium flux reactors ($4 \times 10^{14} \text{ N cm}^{-2} \text{ s}^{-1}$) such as the University of Missouri Research Reactor (MURR, Columbia, MO), Oak Ridge National Laboratory Reactor (HFIR) (Knoxville, TN), the Advanced Test Reactor (Idaho Falls, ID), National Research Universal reactor (NRU) (Canada), Polatom (Poland), BR2 (Belgium), High Flux Reactor (HFR) (Netherlands), FRM2 (Germany), Safari (South Africa), Opal (Australia), and others.

4. THERANOSTICS

Molecular imaging probes are a special class of pharmaceuticals that target specific biochemical signatures associated with disease and allow for noninvasive imaging on the molecular level. Because changes in biochemistry occur before diseases reach an advanced stage, molecular imaging probes make it possible to locate and stage disease, select patients based on predicted response, and track the effectiveness of drugs during treatment. The aim of theranostics is to develop diagnostic tests to screen a disease state directly linked to the application of specific therapies to improve efficacy and cost effectiveness. Before treatment, imaging allows for the personalized diagnosis of the patient's disease by determining the specific phenotype on the molecular level. Additionally, and unlike traditional *in vitro* methods, it can assess the heterogeneity of the diseased tissue or tumor. In theranostics, molecular targeting agents are used to perform initial low dose imaging to evaluate the biodistribution, dosimetry, dose-limiting organ or tissue, maximum tolerated dose (MTD), receptor expression and capacity, and clearance.⁶ The maximum tolerated dose is the highest possible dose of a drug or treatment that does not cause unacceptable side effects. Dosimetry is the calculation of the absorbed dose to tissue from the administered radioactivity. This information can then be used to identify the appropriate molecular targets in diseased tissue that can be targeted with the optimal ligand and radionuclide to deliver tailored individual therapies with the most effective dose.⁷ In the case of nuclear medicine, the term theranostics often refers to using a targeting vector labeled initially with a diagnostic radionuclide to assess the disease followed by personalized treatment using the same targeting vector labeled with a therapeutic radionuclide.

5. RADIONUCLIDES FOR IMAGING AND THERAPY

The majority of radionuclides having nuclear properties suitable for imaging and therapy are metals (e.g., $^{99\text{m}}\text{Tc}$, ^{111}In , ^{90}Y , ^{177}Lu) and require the coordination of chelates to form

complexes with the appropriate biological targeting properties. Each metal is unique and is defined by its oxidation state, coordination number, hard–soft characteristics, kinetic inertness or lability, and redox stability. The transition metals (d-block metals) tend to form mainly octahedral complexes to satisfy their coordination spheres, and thus tetradeятate to hexadentate chelates are often used for the development of potential radiopharmaceuticals based on these radiometals (e.g., $^{99\text{m}}\text{Tc}$, ^{188}Re , ^{64}Cu , ^{105}Rh). The lanthanides tend to form primarily eight to nine coordinate complexes and their binding is ionic in character. The lanthanides are hard metal centers and octadentate carboxylate-containing chelates are generally employed for the radiolanthanides (e.g., ^{177}Lu , ^{153}Sm) to satisfy their coordination requirements and form kinetically inert complexes. In addition to complexing the radiometal in a kinetically inert environment, the chelate often has the dual function of also covalently bonding to the biological targeting vector (i.e., peptide, hormone, or antibody) for directing the radiopharmaceutical to its *in vivo* site, such as tumors. The particular coordination chemistry specific to each radiometal is discussed in the following sections on the radiometals themselves.

5.1. Gold-198

Gold belongs to group 11 of the periodic table and has a Pauling electronegativity of 2.54. Gold as Au(0) is very inert and stable in aqueous solutions, unlike Au(III), which undergoes hydrolysis forming precipitates that are difficult to work with. The atomic radius of Au(I) is 1.51 Å and that of Au(III) is 0.99 Å. Gold has been used medicinally as an antiarthritic drug in the form of chloro(triethylphosphine) Au(I) and Au(I) thiomalate. While the drugs are quite effective, the gold in these compounds is redox active and tends to accumulate in the body, resulting in toxic side effects. This effect is exacerbated in smokers, who have increased cyanide in their bloodstream. Gold-198 is a reactor-produced radionuclide with a half-life of 2.7 days. It emits a β^- particle with a maximum energy of 0.96 MeV (99%) suitable for therapeutic applications and a 412 keV (95.6%) γ -ray that can be used for imaging and localization in biodistribution studies. Gold-198 can be produced by direct irradiation of natural gold foil or metal by the reaction $^{197}\text{Au}(n,\gamma)^{198}\text{Au}$, but only a small fraction of the gold atoms is converted to ^{198}Au , leaving the majority of the target material nonradioactive. The gold target can then be dissolved in aqua regia (3:1 HCl/HNO₃) and partially evaporated to yield HAuCl₄ in dilute HCl (normally 0.05 M). The AuCl₄⁻ can be extracted into organic solvents such as chloroform, dichloromethane, or ethyl acetate as its tetrabutyl ammonium salt, TBA(AuCl₄), allowing for reactions in organic solutions.⁸ The tetradeятate Schiff base ligands (sal₂en, sal₂pn) were shown to form [$^{198/199}\text{Au}-(\text{sal}_2\text{pn})$]PF₆ in 95–100% yield

when heated with NH_4PF_6 in a solution of dichloromethane and ethanol at 40 °C.⁸ Several water-soluble phosphine ligands (THP, HMPE, and HMPB, Figure 1) were evaluated with gold and found to form Au(I) complexes on the macroscopic scale with a tetrahedral geometry.⁹ The ^{198}Au complexes formed on the radiotracer level were evaluated for stability *in vitro* by cysteine challenge and were shown to be stable. Based on these results, biodistribution studies were performed *in vivo* in rats.^{9,10} Significant retention in the blood and carcass was observed for ^{198}Au -THP and ^{198}Au -HMPE indicating *in vivo* decomposition and transchelation to SH groups on proteins *in vivo*. The ^{198}Au -HMPE showed efficient clearance from the blood that was equally divided between urinary and hepatobiliary routes. High-performance liquid chromatography (HPLC) results indicated that the complex was excreted intact in the urine.¹⁰ The high stability observed for these polydentate hydroxymethylphosphine groups suggests that multidentate versions may result in high-stability compounds of Au that could be used for imaging and therapeutic applications.

The bis(thiosemicarbazones) shown in Figure 2 were evaluated with Au(III) as potential therapeutic agents.¹¹ Ligand

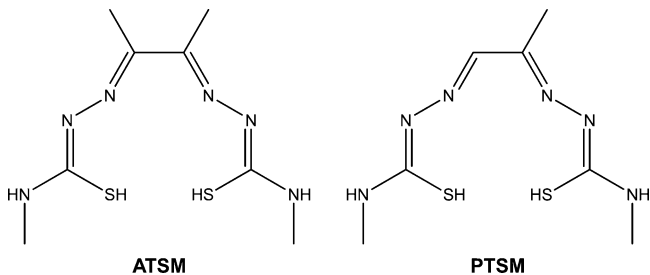


Figure 2. Structures of bisthiosemicarbazone ligands ATSM and PTSM.

systems containing an ethyl, propyl, or butyl backbone between the two imine N donors were synthesized to evaluate chelate ring size effects on the resultant Au(III) complex stability at the macroscopic and radiotracer levels. The complexes were synthesized on the macroscopic scale and fully characterized. The complexes were further radiolabeled with ^{198}Au and evaluated for *in vitro* stability in phosphate-buffered saline at pH 7 and 37 °C. One of these complexes [$^{198}\text{Au}-(3,4\text{-HxTSE})$]⁺, showed high *in vitro* stability and was further evaluated *in vivo* in normal mice.¹¹ The results indicated low *in vivo* stability for [$^{198}\text{Au}-(3,4\text{-HxTSE})$]⁺ but suggested that modifications to the backbone ligand structure allowing for the larger size of Au(III) would likely increase stability.

Recently, there has been widespread interest in designing and developing well-defined ^{198}Au -nanoparticles for tumor therapy applications. Two different synthetic methodologies have been developed, and the therapeutic efficacies of these nanoparticles in animal models have been published.¹² A major advantage of nanosized radioactive particles is their potential to contain numerous radioactive atoms within a single nanoparticle (Figure 3). Delivery of a high therapeutic payload to tumors can be achieved by this method. Gold nanoparticles (AuNPs) have been around for quite some time, but their harsh production methods with toxic chemicals have prevented them from being easily attached to biomolecules for *in vivo* evaluation. New methods to produce AuNPs in aqueous solutions amenable to use in biomolecular applications are being developed.¹³

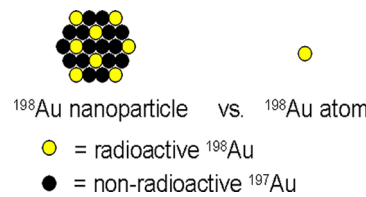


Figure 3. Schematic of gold nanoparticles made with ^{198}Au showing that more radioactive ^{198}Au is delivered per particle compared with a single ^{198}Au .

Balogh and co-workers have utilized a nanocomposite device (NCD) for encapsulation of radioisotopes, providing defined size and surface properties.¹⁴ By this method, the number of radioactive gold atoms can be increased without destroying the targeting ability of the NCD. Gold NCDs are synthesized as monodispersed hybrid nanoparticles composed of radioactive guests immobilized by dendritic polymer hosts. In order to generate nanoparticles, commercially available polymers including polyamidoamine (PAMAM) dendrimers and tecto-dendrimers (composed of a core that can be used to trap a therapeutic agent surrounded by dendrimers) are used as nanocomposites. The synthesis of ^{198}Au nanoparticles by this method involves encapsulation of ^{198}Au within PAMAM dendrimers, which is achieved by mixing dilute solutions of PAMAM dendrimer with an aqueous solution of HAuCl_4 . Salt formation between the tetrachloroaurate anions and the dendrimer nitrogens ensures effective encapsulation of gold within the dendrimer matrix. Upon encapsulation, elemental gold is converted into ^{198}Au within the dendrimer matrix by direct neutron irradiation. A study in a mouse model showed that intratumoral injections of 2.74 MBq (74 μCi) of poly[$^{198}\text{Au}(0)$] with a diameter of 22 nm resulted in a 45% reduction in tumor volume compared with untreated mice, thereby demonstrating their potential in radiotherapy.^{12b}

A different approach for AuNP synthesis consists of using THPAL, a trimeric phosphinoalanine, $\text{P}(\text{CH}_2\text{NHCH}(\text{CH}_3)\text{COOH})_3$, to reduce gold salts in aqueous solutions containing stabilizers, which coat the surface of the AuNPs and form 12–15 nm sized AuNPs with a hydrodynamic diameter of 60–85 nm.¹³ The methods have been modified to allow for formation of both ^{198}Au and ^{199}Au nanoparticles and have also been shown amenable to formation with other coinage metals such as palladium and silver. Gum arabic coated gold nanoparticles (GA- ^{198}Au NPs) were the first and are the most studied nanoparticles to date.^{12a} The reaction consists of heating water containing gum arabic, adding gold either as the NaAuCl_4 salt or the HAuCl_4 acid along with THPAL, which changes from a pale yellow solution to red burgundy. Quality control has shown that this method results in 99% yields. This formulation was evaluated in severe combined immunodeficient (SCID) mice bearing induced human prostate tumors. Tumors received a 70 Gy dose by administering 15 MBq (405 μCi) of the GA- ^{198}Au NPs. An overall 82% reduction in tumor volume was noted between the mice receiving the GA- ^{198}Au NPs and controls receiving saline injections or nonradioactive GA-AuNPs. Biodistributions showed a reduction of gold nanoparticle uptake in the tumor from 70% injected dose (ID) at 24 h to 20% at 30 days postinjection. Based on these results, GA- ^{198}Au NPs are being evaluated for their therapeutic efficacy in canines with spontaneous prostate cancer to aid in translation to humans, since prostate cancer in dogs has been

shown to mimic that observed in humans on the functional level.

A receptor-targeted approach was developed using epigallocatechin-gallate (EGCg).¹⁵ This method proved much simpler because the nanoparticles could be formed at room temperature and EGCg not only achieved reduction of the gold but also served as a stabilizing agent, resulting in an EGCg-conjugated gold nanoparticle (EGCg-¹⁹⁸AuNPs) formulation in a few minutes at room temperature in water. Additionally EGCg targets the laminin receptor Lam 67R, which is overexpressed on human prostate cancer cells.¹⁶ Biodistribution of EGCg-¹⁹⁸AuNPs were evaluated in SCID mice bearing human prostate cancer tumors and were shown to have higher tumor retention than the gum arabic gold nanoparticles and to clear with time.¹⁵ Based on these results, they were evaluated in therapy trials with SCID mice bearing human prostate cancer. Due to the higher initial uptake, only a third of the activity (5 vs 15 MBq, 136 vs 405 μ Ci) for the gold nanoparticles formed with gum arabic) needed to be injected to give a 70 Gy dose.¹⁷ The EGCg-¹⁹⁸AuNPs were shown to be more stable over time, remaining in solution far longer than their gum arabic analogs, and results showed similar reduction of tumor volumes (80% compared with 82%) with higher clearance from normal tissues except for the liver. Due to the similar results with a smaller dose, these EGCg-¹⁹⁸AuNPs will also be evaluated in canines with spontaneous prostate cancer.

Selective targeting has also been evaluated by conjugating the 14 amino acid peptide bombesin (BBN) to the gold nanoparticle surface.^{12a,18} Bombesin targets the gastrin-releasing peptide (GRP) receptors that are up-regulated in a variety of cancers, predominantly breast, prostate, pancreatic, and lung cancers.¹⁹ *In vitro* receptor binding studies have shown a high affinity of BBN-conjugated ¹⁹⁸AuNPs for the GRP receptor in PC-3 cells.^{12a} This conjugate (BBN-¹⁹⁸AuNPs) was evaluated in SCID mice bearing human prostate PC-3 cells and in a spontaneous model of prostate cancer in the transgenic adenocarcinoma of the mouse prostate (TRAMP) mouse. Although the initial studies in PC-3 cells hinted at selective uptake, a more thorough evaluation in which the uptake was compared with ⁶⁴Cu-NOTA-8-Aoc-BBN(7–14)NH₂ showed only nonselective uptake.²⁰ Due to the less than optimal biodistribution, studies are ongoing to develop further analogs of these BBN-containing molecules with linkers that may aid in the selective uptake of these agents.

5.2. Gold-199

Gold-199 is formed by double neutron capture on ¹⁹⁷Au (¹⁹⁷Au(n, γ)¹⁹⁸Au(n, γ)¹⁹⁹Au) resulting in a mixture of the two radioactive gold radionuclides, ¹⁹⁸Au and ¹⁹⁹Au, along with the target ¹⁹⁷Au. Radioactive gold and other radionuclides can be produced by indirect methods, such as neutron capture followed by β^- decay of the parent radioisotope to generate the desired daughter radioisotope. For example, neutron activation of enriched ¹⁹⁸Pt produces ¹⁹⁹Pt (30.8 min half-life), which is followed by β^- decay to ¹⁹⁹Au: ¹⁹⁸Pt(n, γ)¹⁹⁹Pt(β^-)¹⁹⁹Au.

When the indirect method of production is used, separation of the daughter material from the parent is possible, with the distinct advantage that nearly all of the daughter atoms produced are radioactive. A higher specific activity increases radionuclide delivery (i.e., dose) to the tumor, which is especially important when receptors are present in relatively low quantities. Lower specific activity radionuclides such as

¹⁹⁸Au contain a high percentage of nonradioactive atoms and therefore require use of higher amounts of peptide to incorporate the desired amount of radioactivity to bind to the receptor sites. The higher specific activity ¹⁹⁹Au should require less peptide and could result in higher tumor doses. A high specific activity is also important if the targeting molecule is toxic in high concentrations.

Interest in ¹⁹⁹Au was initially due to its ability to form clusters of 11 gold atoms that could then site-selectively attach to monoclonal antibodies.²¹ Recently interest in ¹⁹⁹Au is due to the wide investigation of gold nanoparticles and the ability to use ¹⁹⁹Au in planar (single photon imaging with no reconstruction) and SPECT imaging to study the biodistribution and clearance of agents as well as to assess the dosimetry and MTD of therapeutic gold agents.

5.3. Rhodium-105

Rhodium is a member of the platinum group, in particular a member of group 9. It has a radius of 0.81 Å and a Pauling electronegativity of 2.28. Rhodium in oxidation state +3 is kinetically inert. Rhodium-105 is an attractive radionuclide for potential theranostic applications. In addition to emitting moderate energy β^- particles (0.566 and 0.248 MeV) that can result in cancer cell sterilization or death, it emits low abundance γ rays at 319.2 (20%) and 306 (5%) keV that allow for *in vivo* tracking. The 35.4 h half-life of ¹⁰⁵Rh is sufficient for the synthesis and shipment of potential radiopharmaceuticals, such as radiolabeled peptides. Rhodium-105 was first suggested for use as a therapeutic radionuclide by Troutner because of its moderate energy β^- and γ emissions that allow for imaging and half-life that allows for synthesis and shipping and because it can be obtained non-carrier-added.²² Rhodium-105 is available in very high specific activity by indirect methods from irradiation of an enriched ¹⁰⁴Ru target and also as a fission product from direct neutron irradiation of uranium-235.

Rhodium-105 is produced and purified by a refinement of the method originally developed by Troutner et al.,²² ¹⁰⁴Ru(n, γ)¹⁰⁵Ru(β^-)¹⁰⁵Rh. An enriched ¹⁰⁴Ru target is irradiated with thermal neutrons to produce ¹⁰⁵Ru, which then β^- decays to ¹⁰⁵Rh with a 4.4 h half-life. The Ru target is then oxidized to RuO₄ with sodium hypochlorite, and the RuO₄ is distilled into an HCl trap, leaving the ¹⁰⁵Rh in an oxidation state of +3. The ¹⁰⁵Rh produced is then heated with dilute HCl giving a solution of Rh(III)-chloride.²³

A combination of its nuclear properties and the kinetic inertness of low-spin, d⁶ Rh(III) complexes make ¹⁰⁵Rh attractive for therapeutic applications. Early studies investigating ¹⁰⁵Rh involved complexes formed with nitrogen and oxygen donor ligands, such as amine-oxime,²⁴ amine-phenol,²⁵ amine, and porphyrin²⁶ ligands. However, these ligands required harsh complexation reactions (reflux at high temperatures) and often did not generate high yield products, although the ¹⁰⁵Rh complexes produced were stable and kinetically inert.

Tetradentate thioether ligands have been complexed with ¹⁰⁵Rh and evaluated for their utility as potential radiotherapeutic agents. The macrocyclic S₄-ane ligand, 1,5,9,13-tetrathiacyclohexadecane-3,11-diol ([16]aneS₄-diol),²⁷ and the linear S₄ chelates (2,5,8,11-tetrathiadodecane-1,12-dicarboxylic acid, 2,5,9,12-tetrathiatriadecane-1,13-dicarboxylic acid, 1,14-diphenyl-2,6,9,13-tetrathiadecane, and 2,6,10,14-tetrathiapentadecane-1,15-dicarboxylic acid) with varying backbone

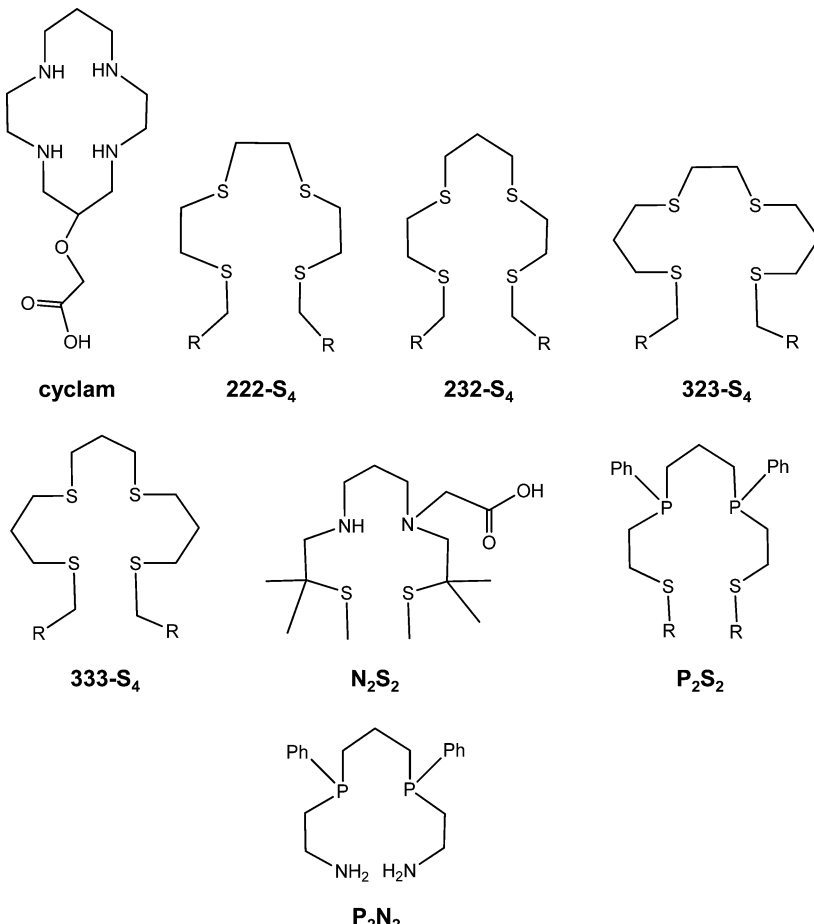


Figure 4. Structures of rhodium ligands cyclam, 222-S₄, 232-S₄, 323-S₄, 333-S₄, N₂S₂, P₂S₂, and P₂N₂.

lengths (222, 232, 323, and 333)²⁸ formed octahedral Rh(III) complexes of the *cis* or *trans* geometry, depending on the chelate ring size (Figure 4). The ¹⁰⁵Rh complexes with these tetrathioether chelates were readily formed in high yields (>95%) at pH 4–5 and 80 °C for 1 h.^{27,28b} Various tetradentate nitrogen- and sulfur-containing macrocyclic ligands were complexed with ¹⁰⁵Rh and evaluated *in vitro* for stability and *in vivo* for their biodistribution patterns.²⁹ The more thioether donors present on the ligand in these N and S ligands, the higher the complexation yield with ¹⁰⁵Rh. A pentadentate N₃S₂ bicyclic macrocyclic ligand, 4,10-dithia-1,7,13-triazabicyclo[11.3.3]nonadecane, was found to complex ¹⁰⁵Rh in greater than 98% yield at pH 5 and 80 °C for 1 h. The X-ray crystal structure of the nonradioactive analog showed the Rh(III) complex to have the form [RhCl(N₃S₂)]⁺Cl₂, with the secondary amine *trans* to the chloride ligand.³⁰ Acyclic diamine dithioether chelates of varying backbone length were evaluated for complexation with Rh(III) and found to result in the presence of multiple isomers.³¹

Substitution reactions on the Rh(III) center require *in situ* reduction to Rh(I) for facile ligand exchange followed by air oxidation to yield the desired Rh(III) complex.³² At the radiotracer level, refluxing ethanol has been used for this purpose.^{27,28b,29–31} Since phosphines are both nucleophiles and reducing agents, several bis-phosphine containing chelates (P₂N₂ or P₂S₂, Figure 4) were evaluated for their potential to reduce the temperature and ethanol content needed for complex formation with Rh(III) at the radiotracer level.³³ The presence of the bis-phosphines did indeed allow lower

temperatures (60 vs 85 °C) and lower ethanol concentrations (5% vs 40%) to achieve high radiochemical yields (>90%), but at the expense of higher ligand concentrations (millimolar rather than micromolar). The ideal chelate system remains to be determined; however the tetrathioether chelate systems (acyclic and macrocyclic) may provide the best overall choice at the radiotracer level.

5.4. Lanthanides

The most commonly considered therapeutic radioisotopes, ¹³¹I, ⁹⁰Y, and ¹⁸⁸Re, have distinctively different chemistries with few common characteristics. However, there exists a large class of radioisotopes, the radiolanthanides and their analogs (i.e., M(III) metals), the members of which have varied nuclear properties (most importantly, half-lives and β⁻ energies) yet share many chemical similarities. The lanthanides chemically differ primarily by a decrease in size moving across the series from La to Lu. The predicted stability of lanthanide complexes increases moving across the series from La to Lu, which follows the decrease in ionic radii and denticity required to result in a stable lanthanide complex *in vivo*. This class of radioisotopes provides the basis for a single ligand–metal system that can be attached to most tumor-targeting molecules. While this ligand–metal system could be based on several ligands, the logical choice is 1,4,7,10-tetra-azacyclotetradecane-N,N',N'',N'''-tetraacetic acid (DOTA, Figure 5) and its close analogs, because these macrocyclic chelates form kinetically stable complexes, even under the most stringent conditions.³⁴ The stability constants of various lanthanides and chelates are listed in Table

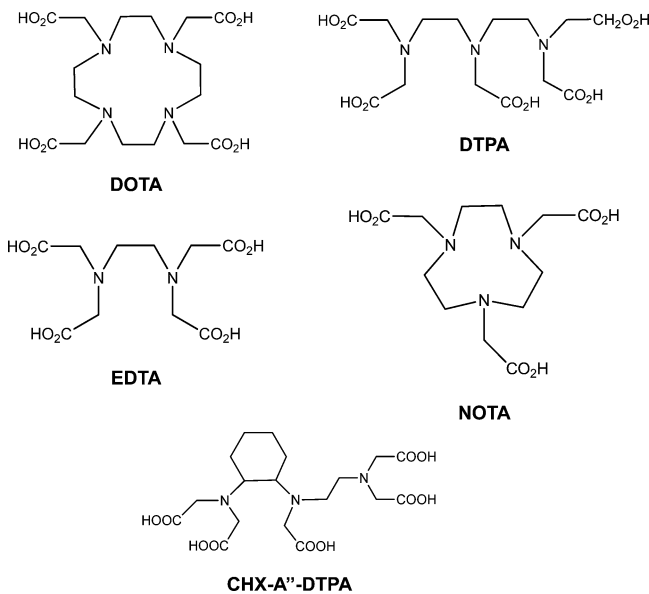


Figure 5. Structures of bifunctional chelator ligands DOTA, DTPA, EDTA, NOTA, and CHX-A''-DTPA.

3. The ultimate success of this approach depends on the biological properties (e.g., specificity, affinity, and blood and

Table 3. Stability Constants, K_{ML}^a , of Metal Complexes.^{69a,151} Letters after the numbers indicate the reference the value was obtained from.

metals	DOTA	NOTA	DTPA	EDTA	TETA
Lu ³⁺	25.5 ^a		22.4 ^b	19.8 ^b	
Ho ³⁺	26.1 ^f		22.7 ^b	18.6 ^b	
Sm ³⁺	26.1 ^f		22.3 ^b	17.1 ^b	15.0 ⁱ
Tb ³⁺	26.2 ^f		22.7 ^b	17.9 ^b	
Pr ³⁺	25.5 ^f		21.1 ^g	16.4 ^b	
In ³⁺	23.9 ^e	25.0 ^e	29.5 ^c	21.0 ^g	21.9 ^f
Ga ³⁺	21.3 ^e	31.0 ^e	25.5 ^c	21 ^e	19.7 ^f
Cu ²⁺	22.2 ^g	21.6 ^e	21.5 ^d	18.8 ^g	21.1 ^c

^a $K_{ML} = [ML]/([L][M])$ where M is a metal ion and L is a ligand.

tumor clearance rates) of the probe. However, the DOTA–M(III) system provides much needed design flexibility in terms of β^- energies, half-lives, and specific activities.

5.4.1. Lutetium-177. Lutetium belongs to the lanthanide group and is the last in the series with the smallest atomic radius (1.0 Å). Its most common oxidation state is +3, and it has a Pauling electronegativity of 1.27 and a coordination number of 9. Lutetium-177 has imageable γ rays [208 (11%) and 113 (6.6%) keV] as well as a low-energy β^- (0.49 MeV) emission, which allows it to be used as both an imaging and a therapeutic radionuclide. The low energy of the β^- particle results in the majority of the dose remaining localized in small areas, which has been shown to be ideal for metastases and in minimizing kidney dose. The 6.64 day half-life is long enough that it can be attached to biomolecules with short or long biological half-lives and allows for distribution to researchers or hospitals in remote regions. Although there are methods that can produce ¹⁷⁷Lu via a cyclotron, it is most commonly produced in a reactor. Due to the large cross section (probability of a neutron interacting with the nucleus) of ¹⁷⁶Lu (2100 b) for the (n,γ) reaction, ¹⁷⁷Lu can be made at

most medium-energy research reactors. There are currently two methods available to produce ¹⁷⁷Lu: direct and indirect. Direct neutron activation of (expensive) isotopically enriched ¹⁷⁶Lu (¹⁷⁶(Lu(n,γ)¹⁷⁷Lu) in a medium flux reactor results in only 20–30% of the ¹⁷⁶Lu atoms being converted to ¹⁷⁷Lu, yielding a specific activity of 740–1110 GBq/mg (20–30 Ci/mg). Higher specific activities can be achieved by irradiation in higher flux reactors such as the HIFR reactor at Oak Ridge National Laboratory, achieving specific activities of 1850–2405 GBq/mg (50–65 Ci/mg). A disadvantage of the direct approach is the production of the long-lived impurity ^{177m}Lu with a half-life of 160 days.

Lutetium-177 can also be produced by an indirect method: neutron capture followed by β^- decay of a parent radioisotope to the desired daughter radioisotope. For example, neutron activation of enriched ¹⁷⁶Yb produces ¹⁷⁷Yb (1.9 h half-life), which is followed by β^- decay to produce ¹⁷⁷Lu, ¹⁷⁶Yb-(n,γ)¹⁷⁶Yb(β^-)¹⁷⁷Lu. As discussed for ¹⁹⁹Au above, separation of the daughter material from the parent is possible with the indirect method and comes with the distinct advantage that nearly all of the lutetium atoms produced are radioactive. Further, the indirect production route does not produce the long-lived ^{177m}Lu impurity because the β^- decay has no branching through the metastable isomer. Separation from the Yb target produces a high-specific activity ¹⁷⁷Lu product, on the order of 4107 GBq/mg (111 Ci/mg), which gives a carrier-free product requiring less biolocalization agent to achieve a given patient dose (because there are fewer nonradioactive lutetium atoms competing with ¹⁷⁷Lu).

It has been estimated that 60–75% of patients diagnosed with breast and prostate cancer will eventually develop bone metastases. These metastases are extremely painful and result in a low quality of life. Radionuclides that mimic calcium or that are bound to bone seeking phosphorus chelators have been developed and used to palliate the pain associated with metastatic bone disease. Radionuclides chosen need to have β^- emissions that are relatively low to minimize bone marrow ablation, which can lead to loss of immunity. Lutetium-177 is a promising radionuclide for bone pain palliation due to its low-energy β^- emission, long half-life, and ability to be produced in large quantities at most medium flux reactors. Lutetium-177 complexed to both ethylene diamine tetramethylene phosphonate (EDTMP) and 1,4,7,10-tetraazacyclododecane-1,4,7,10-tetramethylene-phosphonate (DOTMP) is being evaluated for bone pain palliation.³⁵ A study comparing ¹⁷⁷Lu-DOTMP to ¹⁵³Sm-EDTMP showed that little to no toxicity was observed for the ¹⁷⁷Lu agent when administered to give the same skeletal dose as the ¹⁵³Sm agent, indicating larger ¹⁷⁷Lu doses could be given that may result in longer remission times.³⁵ Clinical trials are ongoing through IAEA coordination evaluating ¹⁷⁷Lu-EDTMP. A scan showing the bone uptake observed for ¹⁷⁷Lu-EDTMP giving a dose of 0.88 GBq (23.7 mCi) and imaged at 7 days is shown in Figure 6.³⁶

Somatostatin receptor targeted therapy of neuroendocrine tumors with ¹⁷⁷Lu-labeled analogs DOTATOC and DOTATATE was investigated after patients treated with ⁹⁰Y-DOTATOC began showing signs of kidney toxicity with the expectation that a lower energy β^- emitter such as ¹⁷⁷Lu may result in lower kidney doses. This led to a 30% objective response with a survival benefit of 40–72 months. Patients are typically given four cycles of 7.4 GBq (200 mCi) of ¹⁷⁷Lu-DOTATATE over a 6–10 week period. Shown in Figure 7 is the Lu-DOTATATE analog. Most clinics perform an initial

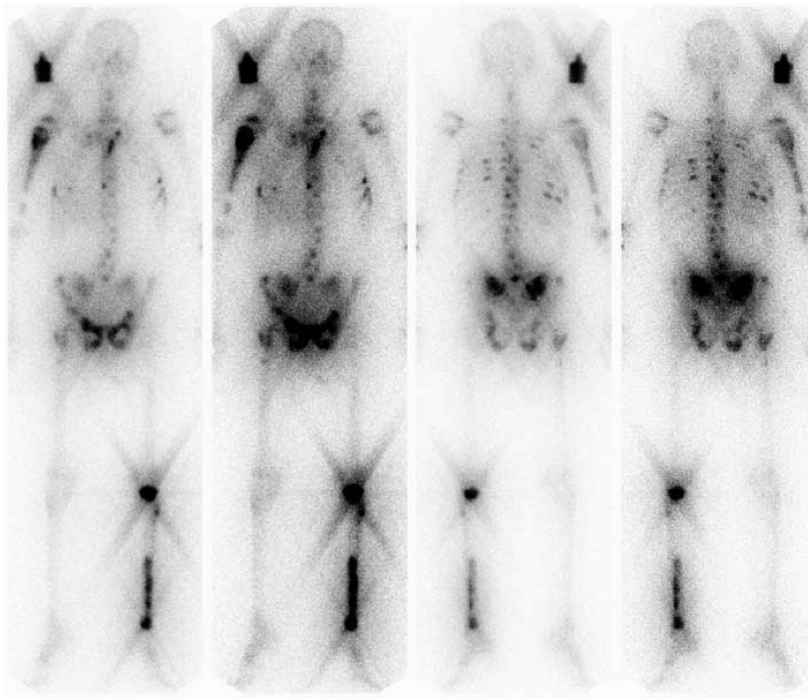


Figure 6. SPECT image of a patient 7 days after receiving 0.88 GBq/kg of ^{177}Lu -EDTMP for palliation of pain due to metastatic bone cancer.

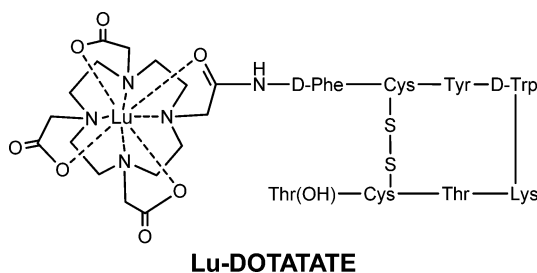


Figure 7. Structure of Lu-DOTATATE.

imaging study with either ^{111}In -Octreoscan or a ^{68}Ga -labeled octreotide analog. However, due to the efficacy of the imaging obtained with ^{177}Lu , some clinics are performing their initial scan with the ^{177}Lu complex itself.

J591, an antibody that targets the antiprostate membrane antigen (PSMA) in androgen-independent prostate cancer has been radiolabeled with ^{177}Lu and evaluated through phase II clinical trials. Shown on the left in Figure 8 is an image of a patient in which the patient was administered 740 MBq (20 mCi) of $^{99\text{m}}\text{Tc}$ -MDP imaged at 2–3 h postinjection showing the metastatic sites in the bone. Shown on the right is the same patient 7 days after injection with 2.59 GBq/m 2 (70 mCi/m 2) of ^{177}Lu -J591 showing the uptake in the prostate and at the metastatic foci in the bone (shown by the red arrows). This scan shows the imaging that can be obtained with ^{177}Lu even a week postinjection. The MTD was determined to be 2.6 GBq/m 2 . Patients were shown to tolerate multiple doses of 1.1 GBq/m 2 .³⁷ Plans are underway to start a phase III trial, and an additional trial is underway in which ^{177}Lu -J591 is given in combination with the chemotherapy drug ketoconazole.

In addition to somatostatin, several analogs of bombesin (BBN) have been radiolabeled with ^{177}Lu and evaluated for therapy of prostate cancer. The one that has been taken the farthest in the clinic for therapy is ^{177}Lu -AMBA.³⁸ A problem

encountered with these peptides is toxic side effects if given in large enough doses; thus labeling in high specific activity appears to be a requirement with these peptides. New BBN analogs have been developed that show better tumor targeting with less normal tissue retention, especially for the antagonists.³⁹ These new antagonists show promise for potential use in radionuclide targeted therapy. Based on the promising results observed for these agents and the low toxicity profiles observed, particularly with ^{177}Lu , a number of peptides and antibodies are being evaluated with ^{177}Lu and more are expected to enter the clinic.

Pretargeting methods have been developed that decouple the delivery of the protein from the radioactivity. The antibody protein is conjugated with a tag or artificial receptor that binds with high affinity to a small molecular probe. This gives the protein targeting agent time to localize to the tumor at a higher concentration before delivery of the radioactivity. Once the antibody has reached maximum uptake at the tumor and clearance from the blood, a smaller molecular probe containing the radioactivity is then injected that binds with high affinity to the tag or receptor on the antibody protein prelocalized on the tumor cells. The small radiolabeled molecule binds rapidly and with high affinity to the receptor antibody, with the remaining unbound fraction excreted rapidly via the kidneys resulting in a high dose to the tumor and minimal dose to the blood and normal organs. The outcomes of these methods are a higher dose delivery to the tumor (typically 10-fold improvement) compared with direct radiolabeled monoclonal antibodies (mAB), increased therapeutic efficacy, and minimal dose and thus toxicity to normal tissues such as the blood and bone marrow.

Most strategies for pretargeting are based on high-affinity biological recognition systems such as mAB/hapten, or biotin/avidin or streptavidin, which suffer from immunogenicity, inducing immune responses as they are recognized by the body's defense system. This precludes them from being used in

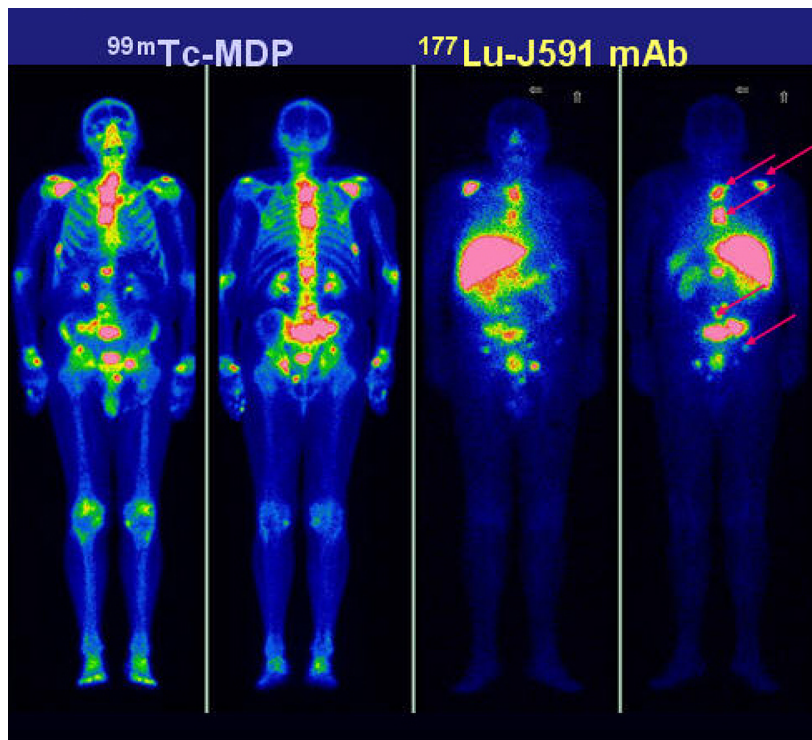


Figure 8. Shown on the left is a SPECT image of a patient with androgen-independent prostate cancer 2–3 h after injection of 740 MBq of $^{99\text{m}}\text{Tc}$ -MDP showing the metastatic foci in the bone. Shown on the right is the same patient 7 days after injection with 2.59 GBq/m² of ^{177}Lu -J521 showing the uptake in the prostate and at the metastatic sites in the bone (shown by red arrows).

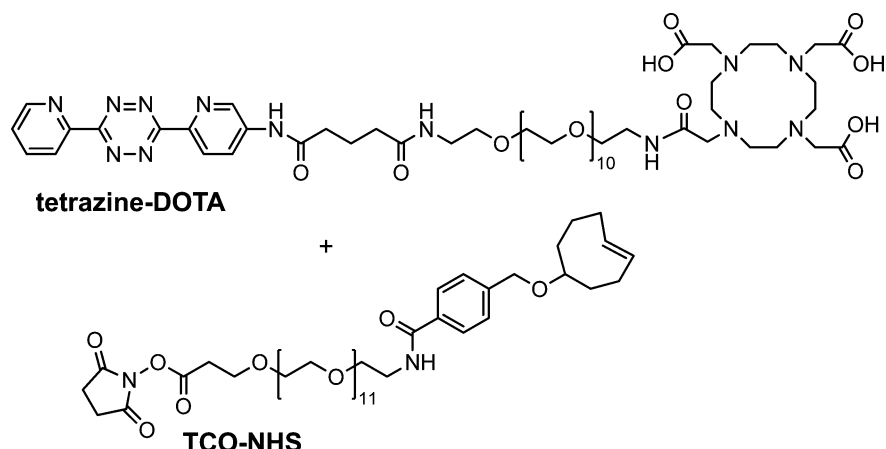


Figure 9. Structures of bioorthogonal pretargeting molecules tetrazine–DOTA and TCO–NHS.

repeat or dose fractionation treatments, which have demonstrated maximum efficacy for a variety of cancer treatments including external beam therapy, chemotherapy, and radioimmunotherapy (RIT).

A novel pretargeting method has been developed that uses a bioorthogonal chemical reaction, instead of biological components, to bind the small radiolabeled probe with high affinity to the tumor-bound antibody. The approach is based on the Diels–Alder reaction between a tetrazine–DOTA analog (shown in Figure 9), which demonstrates high thermodynamic and chemical stability with most metals and a strained *trans*-cyclooctene (TCO) derivative (Figure 9) conjugated to the anti-TAG-72 mAb CC49 through a lysine residue. This reaction was chosen based on its high second-order rate constant of $13090 \pm 80 \text{ M}^{-1} \text{ s}^{-1}$ at 37 °C in phosphate-buffered

saline.⁴⁰ CC49 was chosen due to its high affinity to TAG-72, an antigen with limited internalization and shedding that is overexpressed in a wide range of solid tumors including colon cancer.^{41,3} The initial *in vivo* proof-of-principle imaging studies were performed in mice bearing colon cancer xenografts that were administered 100 µg of TCO–CC49, followed one day later with 3.4 equiv of ^{111}In -DOTA–tetrazine, (42 MBq, 1.13 mCi).⁴⁰ The animals were imaged 3 h later, and the tumor was shown to have a 4.2% ID/g and a tumor to muscle ratio of 13:1.⁴⁰ Besides the tumor, the bulk of the activity was found in the bladder, with a small amount in the kidney and some residual found in the liver and blood that was attributed to circulating TCO–CC49. Controls were performed in which the unmodified CC49 and TCO-modified rituximab, which has no affinity for TAG-72, were injected in place of TCO–CC49. No

tumor uptake was observed in either case, supporting the antigen-specific binding of CC49–TCO with ^{111}In -DOTA–tetrazine.⁴⁰ Following these promising results, the TCO–CC49/DOTA–tetrazine pretargeting method was further optimized (e.g., dosing and timing of radiolabeled probe) and evaluated against the direct labeling DOTA–CC49 method with the therapy radioisotope ^{177}Lu in biodistribution studies with the same mouse model of disease.⁴² Using the biodistribution data obtained, the estimated maximum deliverable dose to the tumor without being lethal to marrow was nearly 5 times higher with the pretargeting method at 80 Gy than the subtherapeutic dose of 17 Gy for the direct labeling method.⁴²

5.4.2. Samarium-153. Samarium is also a member of the lanthanide series with an ionic radius of 1.10 Å and a Pauling electronegativity of 1.17. Radioisotopes of Sm can be produced via reactor or accelerator. The most common radioisotope, ^{153}Sm , has a half-life of 46.27 h and emits β^- particles with a maximum energy of 0.8 MeV and a mean energy of 0.23 MeV, with an average soft-tissue range of 0.3 mm. It emits an imageable γ ray of 103 keV (28.3%), which can be used for monitoring distribution as well as calculating dosimetry. It is produced by neutron irradiation of an enriched ^{152}Sm target, $^{152}\text{Sm}(n,\gamma)^{153}\text{Sm}$. The target is normally irradiated as the oxide or nitrate and then dissolved in dilute hydrochloric acid. The cross section is relatively high (206 b) and produces ^{153}Sm with a specific activity of 222 GBq/mg (6 Ci/mg) when irradiated at a flux of $1.2 \times 10^{14} \text{ N cm}^{-2} \text{ s}^{-1}$ for approximately 155 h.

Samarium complexed with EDTMP (Quadramet), shown in Figure 10, is approved for the palliation of bone pain associated

up to six cycles of low-dose ^{153}Sm -EDTMP have remained pain-free for 6–12 months.⁴⁵

Clinical trials evaluating the combination of Quadramet with chemotherapy using docetaxol and estramustine have been performed in castration-resistant prostate cancer patients and have shown an increase in the progression-free survival of the patients.⁴⁶ Side effects were minimal and results indicated this might be a viable option for patients that should be explored further. Due to its low specific activity, ^{153}Sm has not been evaluated with many of the new molecular selective targeting agents.

5.4.3. Holmium-166. Holmium, also a lanthanide, has a radius of 1.04 Å and a Pauling electronegativity of 1.23. Holmium-166 decays with a half-life of 26.8 h and emits β^- particles with a maximum energy of 1.85 MeV and γ rays with energies of 80.6 (6.2%) and 1379 keV (1.13%). The 80 keV photon is used for imaging, and it is possible to obtain SPECT images of ^{166}Ho radiopharmaceuticals. Additionally, with the use of phantoms, it is possible to obtain reasonable quantification during early FDA-approved IND sponsored clinical trials, and the imaging provides a good estimate of organ and whole body dosimetry. Holmium-166 is routinely made by direct neutron irradiation of ^{165}Ho , which is 100% abundant, $^{165}\text{Ho}(n,\gamma)^{166}\text{Ho}$.

Production via this route results in a low specific activity material because only a very small portion, 0.31%, is actually converted to ^{166}Ho . The radionuclide thus produced has seen applicability in nuclear medicine, but its agents contain macroscopic quantities of nonradioactive ^{165}Ho isotopes and thus have comparatively low specific activities. In nuclear medicine, the use of high specific activity radionuclides is generally preferred so that the finite binding sites for biolocalization agents are occupied with the maximum amount of the medically desired radionuclide.

Another mode of ^{166}Ho production exists via an indirect route. In this method, an enriched ^{164}Dy target undergoes a $(2n, \gamma)$ reaction to produce ^{166}Dy that subsequently decays by β^- emission to the desired ^{166}Ho product: $^{164}\text{Dy}(2n, \gamma)^{166}\text{Dy}(\beta^-)^{166}\text{Ho}$. Double neutron capture reactions typically are not favorable; however, in this case the neutron absorption cross sections of ^{164}Dy and ^{165}Dy have been experimentally shown to produce up to 1 Ci of ^{166}Ho per milligram of ^{164}Dy . The specific activity of ^{166}Ho produced using this route can be much higher than that of ^{166}Ho produced by direct irradiation, if a chemical separation of ^{166}Ho from the ^{164}Dy target material is achieved. The first neutron capture cross sections are effectively 2731 b thermal and 932 b epithermal to form ^{165}Dy with a half-life of 2.33 h. Although the half-life of this intermediate is relatively short, ^{165}Dy has thermal and epithermal neutron capture cross sections of 3600 and 22000 b, respectively, and thus a significant percentage of ^{165}Dy atoms capture a second neutron to form ^{166}Dy . One milligram of enriched ^{164}Dy irradiated over 155 h at a thermal flux of 4×10^{14} neutrons $\text{cm}^{-2} \text{ s}^{-1}$ thermal and an epithermal flux of 1.6×10^{13} neutrons $\text{cm}^{-2} \text{ s}^{-1}$ at the MURR has been shown to produce close to the theoretical yield of 1.2 Ci of ^{166}Dy . A thermal neutron is defined as having an average energy of 0.025 eV, and epithermal neutrons have an energy range from 1 eV to 10 keV.

An example of targeted radiotherapy is skeletal targeted radiotherapy (STR), which used the β^- emitting radionuclide ^{166}Ho coupled to a small-molecule biolocalization agent abbreviated DOTMP (1,4,7,10-tetraazacyclododecane-1,4,7,10-tetramethylenephosphonic acid). The STR treatment

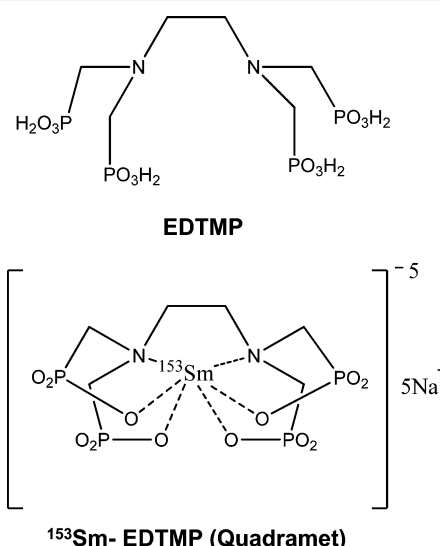


Figure 10. Structures of EDTMP and Sm-EDTMP.

with metastatic disease that is derived from breast, prostate, and lung cancer. As with most bone agents, it exhibits a much higher accumulation in the metastatic lesions (five times higher compared with normal bone).⁴³ Quadramet exhibits a high clearance from the blood and reaches a maximum bone uptake and blood clearance at 6 h postinjection.⁴⁴ The main excretion path is through the kidneys into the urine. Pain relief is normally observed within 2 weeks and persists from 4 to 35 weeks. The main side effects are thrombocytopenia, transient myelosuppression, and a drop in platelet counts, which return to normal typically 10 weeks post-treatment. Patients receiving

using ^{166}Ho -DOTMP targets multiple myeloma, a cancer of the plasma cells (a type of white blood cell), that presents in the bone marrow. Multiple myeloma destroys bone structure, causes anemia, often results in kidney failure, and affects 500 000 people in the U.S. alone, claiming 11 000 lives each year. The conventional chemotherapeutic and total body radiation treatment regimens are only marginally effective, with a five-year survival rate for myeloma patients of only 30%.

Therapy with STR offered a promising and more focused alternative to total body radiation and chemotherapy regimens. Prior to STR treatment, a bone marrow sample was withdrawn from the patient and preserved. The patient would initially receive a small dose and be imaged to determine how that patient handled the drug and the dosimetry to the bone and kidneys to calculate a patient-specific dose. Imaging methods were shown to be more reliable for assessing patient pharmacokinetics, clearance, and dose.⁴⁷ A week later, the patient would receive a higher dose, calculated based on the imaging of STR, during which the ^{166}Ho -DOTMP adduct accumulates in the bone. The ^{166}Ho , carried to the site by the DOTMP, releases β^- radiation that ablates the bone marrow. This targeted radiotherapy treatment places the radiation where it is the most effective, which results in a minimum amount of damage to normal healthy cells and maximum damage to the bone marrow. After approximately 1 week, the previously withdrawn bone marrow, having been cleansed of cancer cells, is returned to the patient to restore disease free marrow function. The success to date of the phase I/II trials of STR for treatment of multiple myeloma has been extremely positive. NeoRx Corporation has reported that 23 of the 56 patients evaluated after treatment with STR in combination with high dose chemotherapy were in complete remission, and four other patients achieved partial remission.^{47,48}

5.4.4. Terbium-161. Terbium has a radius of 1.06 Å and a Pauling electronegativity of 1.1. Terbium-161 is a particularly attractive radiolanthanide when relatively slow but high tumor uptake is characteristic of the labeled agent and when minimizing kidney toxicity by use of a low-energy β^- emitter is particularly important. Terbium-161 is of interest due to its low-energy γ emissions (48.9 (17%) and 74.6 (10.2%) keV) for intraoperative scanning of somatostatin receptor-positive tumors, wherein a hand-held probe that can detect γ emissions is used to guide the surgeon to the tumor sites to aid in complete removal.⁴⁹ Terbium-161 has a half-life of 6.91 days with low-energy β^- emissions with a maximum of 0.59 MeV and, in contrast to ^{177}Lu , emits a significant quantity of conversion and Auger electrons.⁵⁰ On average, 2.24 Auger and conversion electrons are emitted in addition to the one β^- particle per decay. Thus, ^{161}Tb is potentially useful for radiotherapy using receptor site targeting agents such as monoclonal antibodies and peptides, much in the same manner as ^{177}Lu , particularly if the ^{161}Tb is available no-carrier-added. One route to such high specific activity ^{161}Tb -161 is through neutron irradiation of isotopically enriched ^{160}Gd to produce ^{161}Gd , which rapidly β^- decays (3.7 min half-life) to ^{161}Tb : $^{160}\text{Gd}(n,\gamma)^{161}\text{Gd}(\beta^-)^{161}\text{Tb}$.

Chromatographic separation of the product ^{161}Tb from the target ^{160}Gd is then necessary. Terbium-161 has been produced by different groups and used to radiolabel DOTATATE and compared with ^{177}Lu -DOTATATE.^{50,51} The ^{161}Tb was shown to label similarly to ^{177}Lu , and a biodistribution in mice xenografted with the rat pancreatic tumor AR42J showed similar uptake and clearance properties.⁵¹ Both ^{161}Tb and ^{177}Lu

have half-lives of ~7 days, β^- emissions appropriate for therapy (~0.5 MeV), and γ emissions that enable dosimetry and pharmacokinetic measurements. The ^{161}Tb is prepared in high specific activity and its lower energy γ emission (74.6 keV) is being investigated because it may result in lower dose to normal tissues than that observed for ^{177}Lu .

5.4.5. Promethium-149. Promethium has a radius of 1.11 Å and a Pauling electronegativity of 1.13. Promethium is unique in that there are no stable (nonradioactive) isotopes of Pm. Promethium-149, a high specific activity radiolanthanide with properties similar to ^{153}Sm , has recently been developed and shown promising results.⁵² Just as with ^{177}Lu , ^{149}Pm has an imageable γ emission (286 keV, 3%) and a moderate energy β^- emission of 1 MeV. Chemically, it is very similar to ^{177}Lu and ^{90}Y and therefore can be coordinated to biomolecular targeting systems utilizing the same ligand systems, most notably DOTA.^{52a,53} Promethium-149 is produced by an indirect production route from neutron irradiation of ^{148}Nd to form ^{149}Nd , which β^- decays to ^{149}Pm . Chemical separation of ^{149}Pm from the Nd target material results in high specific activity ^{149}Pm . Particle-emitting radioisotopes linked to somatostatin analogs are being evaluated for radiotherapy. Lower specific activity radionuclides such as ^{153}Sm and ^{177}Lu contain a high percentage of nonradioactive atoms and therefore require higher amounts of targeting vector, which bind to the receptor sites. The higher specific activity ^{149}Pm should require less targeting vector and could result in higher tumor doses. Radiotherapy studies comparing CC49 labeled by conventional and pretargeting methods showed that with pretargeting ^{177}Lu and ^{149}Pm survival rates were indistinguishable.^{52b,c}

5.5. Rhenium-186 and -188

Rhenium is a group 7 congener of Tc and therefore, in many cases, shares remarkably similar chemical behavior to Tc. Technetium-99m is a diagnostic radionuclidic workhorse in nuclear medicine, and a wealth of information exists on its incorporation into biomolecules. Thus, $^{99\text{m}}\text{Tc}$ radiocomplexation knowledge can often be applied to the ^{186}Re and ^{188}Re radionuclides; some even describe $^{99\text{m}}\text{Tc}$ and $^{186/188}\text{Re}$ as a matched pair for radiodiagnostics and radiotherapeutics. However, significant differences between $^{99\text{m}}\text{Tc}$ and $^{186/188}\text{Re}$ complexes do occur, most often involving dissimilarities in their substitution kinetics and redox chemistry.⁵⁴ Rhenium is generally slower to substitute than Tc, which can result in different coordination geometries and ligand patterns. Further, Re is more difficult to reduce and, conversely, easier to oxidize. This difference in redox behavior both reduces the number of readily accessible oxidation states for Re relative to Tc and requires a more reducing environment to prevent oxidative loss of the radiometal from the complex. For example, Benny and co-workers reported differences in Re(V) and Tc(V) Schiff base complexes due to slower substitution rates for Re,⁵⁵ and redox chemistry has limited the direct translation of $^{99\text{m}}\text{Tc}$ pyridyl hydrazine labeling methodologies (i.e., HYNIC-based) to the analogous $^{186/188}\text{Re}$ complexes. In these and other similar cases, radiotechnetium and radiorhenium do not behave as a matched pair.

Fortunately, ^{186}Re and ^{188}Re have potential to stand alone as theranostic radionuclides, due to their decay by both particle and γ emissions. Rhenium-188 has a 17.0 h half-life, a 2.12 MeV β^- emission, and a 155 keV (15%) γ emission. It is obtained from a $^{188}\text{W}/^{188}\text{Re}$ generator with very high specific activity. The ^{188}W parent radionuclide (69.4 day half-life) is produced

by double neutron capture on ^{186}W [$^{186}\text{W}(\text{n},\gamma)^{187}\text{W}(\text{n},\gamma)^{188}\text{W}$] in a high-flux nuclear reactor and is then loaded onto an alumina-based generator. Following β^- decay of the ^{188}W parent radionuclide, the ^{188}Re daughter radionuclide is eluted as radioperrhenate ($\text{Na}^{188}\text{ReO}_4$) in normal saline. This separation of the parent and daughter radionuclides results in near theoretical levels of specific activity for ^{188}Re .

Rhenium-186 has a 3.72 day half-life, a 1.07 MeV β^- emission, and a 137 keV (9%) γ emission. It can be reactor-produced by neutron capture on ^{185}Re to yield a low specific activity product through the $^{185}\text{Re}(\text{n},\gamma)^{186}\text{Re}$ nuclear reaction. Alternatively, ^{186}Re can be accelerator-produced with higher specific activity via proton/deuteron bombardment of tungsten targets, such as $^{186}\text{W}(\text{p,n})^{186}\text{Re}$ using enriched ^{186}W target material. Various accelerator approaches are being explored,⁵⁶ but regular productions have not yet been established. Routine availability of high specific activity ^{186}Re would have a great impact in theranostic research, because its longer half-life would allow the study of slower *in vivo* processes through labeling of biomolecules with longer *in vivo* circulation.

In nuclear medicine applications, Re complexes are typically reported in the +5 and +1 oxidation states, and to a lesser degree +3. With two thermodynamic sinks (ReO_4^- and ReO_2) and a proclivity toward oxidation on high dilution, design of a stable chelate for Re is critical. Should oxidation occur, the body quickly clears ReO_4^- through the renal–urinary system and avoids unwanted accumulation in most nontargeted tissues; blocking agents such as sodium perchlorate or potassium iodide can be administered to prevent the transient uptake of ReO_4^- in thyroid, salivary gland, and stomach tissues caused by their expression of the sodium–iodide symporter for which ReO_4^- is a substrate.⁵⁷ Nonetheless, highly stable and selectively targeted $^{186}/^{188}\text{Re}$ complexes are desired to maximize therapeutic efficacy. A brief summary of Re(V)/Re(I) chemistry and example applications are presented here; more detailed reviews can be found in the literature (e.g., see reviews by Blower⁵⁸ and Donnelly^{54b}).

The +5 oxidation state is the most easily achieved from reduction of the Re(VII) starting material ReO_4^- , which leads to the majority of complexes with Re as Re(V). These complexes typically have square pyramidal geometry, consisting of an N_xS_{4-x} tetradentate chelate surrounding a monooxo Re(V) metal center.⁵⁹ The oxorhenium(V) core can be incorporated through the use of bifunctional chelating agents, like diamine dithiols (DADT) and monoamine monoamide dithiols (MAMA),⁶⁰ or by direct integration into molecules, such as α -melanocyte-stimulating hormone and somatostatin peptide analogues,⁶¹ with the bifunctional chelate approach far more widely used. In either case, the nitrogen donors include either amines or amides or both, while the sulfur donors are typically thiols. Stability against reoxidation is key, and chelates containing two or more sulfur donors (sometimes phosphine donors, also reducing in nature) are used to protect against instability at the radiotracer level *in vivo*. However, the lipophilicity and charge changes imparted to these complexes by additional thiol or phosphine incorporation must be considered during the selection process, to prevent undesirable effects on the pharmacokinetics (e.g., increased hepatobiliary clearance).

The Re(I) tricarbonyl monocationic core has a low-spin d⁶ electronic configuration, making it more kinetically inert than Re(V) and therefore attractive for nuclear medicine applications. This stable core can be obtained as the tricarbonyl triqua-

form $[\text{Re}(\text{CO})_3(\text{OH}_2)_3]^+$ through reduction of perrhenate using a two-step kit formulation developed by Schibli and co-workers,⁶² though the conditions are harsher than those used in IsoLink kits (Mallinckrodt) for the analogous ^{99m}Tc synthon. Substitutions of the coordinated water ligands are facile and are typically carried out with tridentate chelates containing amines, imines, carboxylates, phosphines, thiols, or thioethers. The *fac*- $[\text{Re}(\text{CO})_3]^+$ organometallic synthon is small, which allows its addition to biomolecules of various sizes but also adds considerable lipophilicity to the biomolecule.

Rhenium radiopharmaceuticals have been used in a variety of clinical applications; these include clinical trials for the palliation of pain from bone metastases⁶³ and the treatment of inoperable hepatocellular carcinomas,⁶⁴ advanced lung cancer,⁶⁵ and rheumatoid arthritis.⁶⁶

5.6. Scandium-44 and -47

Scandium chemistry is intermediate between that of Al, Y, and the lanthanides. Scandium(III), with an ionic radius of 0.68 Å, is chemically similar to Y and the heavier lanthanides. It is an electropositive element with a Pauling electronegativity of 1.36. Its chemical behavior is mainly ionic with the most stable cation being Sc(III). Organometallic complexes involving Sc(III) have coordination numbers ranging from 3 to 9; however the most common are the octahedral complexes due to its small ionic radius. Scandium radioisotopes are of interest for both targeted radiotherapy and diagnosis. Scandium-47 has a half-life of 3.35 days and emits both a moderate β^- particle (0.600 MeV, 100%) and an imageable γ ray (159 keV, 68%) comparable to ^{67}Cu , a promising radionuclide for targeted radionuclide therapy. Scandium-44 is a β^+ emitter (632 keV, 94.27%) with energy comparable to ^{18}F but a longer half-life of 3.97 h. Scandium-44 can be used as an imaging surrogate for many +3 metals including the lanthanides and Y by coupling it to the same biological vector and estimating dosimetry for therapy with ^{47}Sc .

Production can be carried out on a cyclotron by irradiation with a proton beam on enriched ^{44}Ca by the nuclear reaction $^{44}\text{Ca}(\text{p,n})^{44}\text{Sc}$ or by proton irradiation of enriched ^{48}Ti by the nuclear reaction $^{48}\text{Ti}(\text{p,2p})^{47}\text{Sc}$. Scandium-47 can be produced in a reactor by indirect methods either by neutron irradiation of enriched ^{46}Ca producing ^{47}Ca , which β decays to ^{47}Sc , or by proton irradiation of enriched ^{48}Ti . The target $^{48}\text{TiO}_2$ is initially dissolved in hot sulfuric acid, dried down, and then dissolved in water containing 0.3% hydrogen peroxide to oxidize Ti to the +4 state, followed by separation as previously described.^{21f} Briefly, the carrier-free ^{47}Sc is separated from the Ti target material by loading on a large cation exchange column in which the Ti is eluted with 1.0 and 2.0 N HCl. The ^{47}Sc is eluted with a mixture of 4.0 N HCl/0.1 N HF. The ^{47}Sc is then evaporated to near dryness initially reconstituted with aqua regia, then twice with concentrated HCl, and last with 30% hydrogen peroxide. The residue is then dissolved in water and loaded onto a second column to remove the final trace amounts of the target material and other trace metal impurities; finally the ^{47}Sc is eluted and dried down as previously described.⁶⁷

A $^{44}\text{Ti}/^{44}\text{Sc}$ generator is possible and production of such a generator has recently been described to produce regular batches of about 2 mCi (74 MBq).⁶⁸ Titanium-44 is produced through the nuclear reaction $^{45}\text{Sc}(\text{p,2n})^{44}\text{Ti}$, which requires a high proton flux (25 MeV proton, 200 μA , long irradiation). Irradiation of 1.5 g of Sc target material produced about 5 mCi (185 MBq).

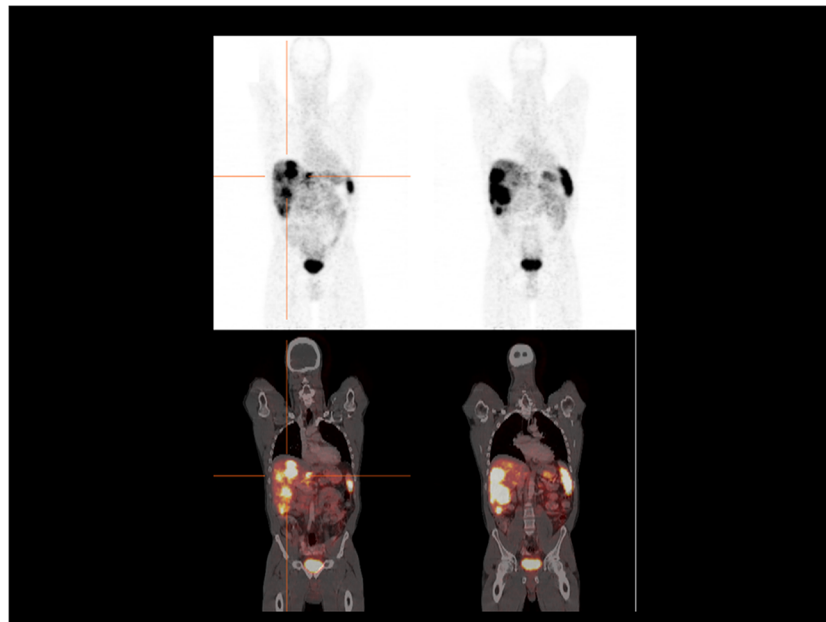


Figure 11. PET/CT image of a patient 19 h after receiving 32 MBq (0.8 mCi) of ^{44}Sc -DOTATOC for imaging of neuroendocrine tumors. The dose was prepared by Frank Roesch at the University of Mainz, Germany, and shipped 300 km to the Theranostics Center at the Zentralklinik in Bad Berka, Germany.

Scandium radioisotopes are of interest for both targeted radiotherapy and diagnosis. For use in nuclear medicine, it is necessary to form ligand complexes endowed with a high kinetic stability. Experimental data on stability constants for the commonly used complexes such as DTPA, DOTA, NOTA, and TETA have long been published and are recognized as reference values. Notably, the chelating ligand DOTA binds transition metals and rare earths with high stability under physiological conditions, leading to its use *in vivo*.⁶⁹

However, for scandium there is no relevant data available in the literature with the exception of the Sc–EDTA system, for which the stability constant was found to be $\log K_{\text{ML}} = 23.1$.⁷⁰ The Sc–DOTA complex was shown to have a coordination number of 8⁷¹ with a square antiprismatic geometry, no apical water molecule, and bond distances of 2.44 Å for Sc–N and 2.15 Å for Sc–O.

The stability of Sc–ligand versus transferrin was monitored by UV. It was shown that the equilibrium was not reversible over the time scale of the experiments for NOTA, DTPA, and DOTA, whereas a fast transfer of Sc to the transferrin occurred for the Sc–TETA complex. The radiolabeling and stability in the presence of a bone substitute and rat serum were studied for the Sc–DTPA and Sc–DOTA systems out to 7 days. It was shown that Sc–DOTA was more suitable from a medical perspective.⁷² Due to its longer half-life, Sc has been evaluated for binding with DOTA-conjugated peptides.⁷³ Work has been done to show that high labeling yields (>98%) can be obtained with DOTATOC and that it remains stable out to at least 25 h even when challenged by ligands such as EDTA and DTPA. Based on these results, ^{44}Sc -DOTATOC was prepared using the $^{44}\text{Ti}/^{44}\text{Sc}$ generator located at the University of Mainz (Mainz, Germany) and shipped 300 km to the Theranostics clinic at the Zentralklinik in Bad Berka (Bad Berka, Germany). A patient was injected with 32 MBq (0.86 mCi), and a PET/CT scan was taken at 19 h postinjection as shown in Figure 11; this was the first human use of ^{44}Sc -DOTATOC in a patient with liver metastases from a neuroendocrine neoplasm. Even at

this late time point, the metastatic foci can be clearly seen. The longer half-life of ^{44}Sc may allow for PET imaging of larger peptides and antibody fragments that are currently limited due to the short half-lives of commonly used PET radioisotopes.

Scandium was shown to be transferred between transferrin and ferritin *in vitro*, although *in vivo* the binding to ferritin appears to be negligible compared with other transition metals.⁷⁴ *In vivo*, transferrin was shown to play a major role in the transport of Sc in the plasma and was the only scandium–serum protein complex observed. It has been reported that Sc(III), Y(III), and La(III) bind to globulin and DNA, and transferrin is a major Sc(III) or Y(III) binding protein in blood plasma.⁷⁵ Hirano has shown that Sc–EDTA was taken up rapidly by the kidneys with subsequent elimination via the urine, while ScCl_3 was deposited extensively in the liver and spleen in mice.

ScCl_3 and Sc–nitrilotriacetic acid (NTA) bind more strongly to α -globulin than to albumin in equilibrium dialysis studies. Although Sc has been shown to bind to the β -globulin fraction *in vivo*,⁷⁶ particularly to transferrin, it can bind to other proteins as well.

Rosoff et al.⁷⁰ have shown that the excretion of Sc-citrate is slightly higher than that of rare earth elements administrated as chlorides in organs such as lung, muscle, and bone. Bone uptake of Sc is about 5%. Since the Sc chelates are excreted readily, the concentration of Sc compounds is low in all tissues. It has been shown that accumulation of Sc(III)-citrate (low stability constant) in the liver, spleen, and bone was much higher than that of Sc(III)-EDTA (high stability constant) following injection in mice. Some authors⁷⁰ have shown that when Sc(III)-NTA (intermediate stability constant) was injected, a relatively high concentration of Sc was accumulated in the bone compared with Sc(III)-citrate or Sc(III)-EDTA.

Moeller⁷⁷ postulated a correlation between the ionic radius of a rare earth and its ability to form stable compounds. Rare-earth chelates with a high stability constant dissociate very little and are rapidly excreted, while those with weak or intermediate

stability constants dissociate more readily, and the rare earth is deposited in tissues and excretion is minimal. *In vitro* studies have shown that the biological behavior of Sc is similar to that of other rare earths; for instance, Sc forms stable complexes with chelating agents of the amine carboxylates.⁷⁸ EDTA and DTPA are both effective in removing Sc from man, and DTPA especially led to a considerable excretion of scandium.⁷⁹

Scandium(III) has the remarkable property of enhancing the tumor/nontumor concentration ratios of intravenously administered ⁶⁷Ga. ⁶⁷Ga-citrate is now in widespread use for the detection of malignancies in man using scintigraphic scanning techniques. In animal studies where the toxicity of Sc was of interest because of its possible use as an augmentative agent for ⁶⁷Ga scanning patients with cancer, Byrd et al. observed that the uptake and retention of Sc in some tissues appeared to be exceedingly prolonged.⁸⁰ Furthermore, in distribution studies involving high specific activity ⁴⁷Sc, they found that the administration of stable Sc had an additional pronounced effect on the retention and tissue distribution of ⁴⁷Sc.

The distribution of high specific activity ⁴⁷Sc in rats appeared to be nonspecific in that few tissues showed any particular preferential affinity for the radionuclide. The spleen is a striking exception. The reason for the high concentration of high specific activity ⁴⁷Sc in the spleen is not apparent, although it does not appear to be due to deposition of colloidal material because other reticuloendothelial tissues did not show high uptake.

A novel pretargeting approach that has been recently developed is that of antibodies that bind DOTA rare earth complexes. Of particular interest is the use of these antibodies to selectively bind DOTA analog complexes of rare earth metals *in vivo* for diagnosis and treatment. Corneillie et al.⁸¹ examined the monoclonal antibody 2D12.5 developed against the DOTA analog NBD ((S)-2-(4-nitrobenzyl)-DOTA). They found that 2D12.5 bound not only Y-NBD but also NBD complexes of all lanthanides. The NBD chelate bound to the group 3 ion Sc(III) binds to the antibody with a much lower affinity (<1%) than the strongest binding rare earth complexes, perhaps because Sc(III) has a much smaller ionic radius.⁸²

Additional work done by Corneillie et al.⁸³ showed that the 2D12.5 fragment antigen binding (Fab)-metal complex was bound nonselectively for two reasons. All DOTA complexes with rare earth elements, because of their chemical and physical similarities, were bound with comparably high affinities to the antibody. Because there is no direct protein–metal interaction, the binding interactions between the antibody and the metal–DOTA complex are only indirectly affected by changing the metal. The second reason for the nonselective binding results from the symmetrical approximately cylindrical nature of the DOTA chelate, which places heteroatoms in approximately the same relative position regardless of the metal–DOTA moiety. However, this nonselectivity apparently does not extend to metals other than Y and the lanthanides; while the binding constants of the latter DOTA complexes to 2D12.5 Fab antibody vary by less than a factor of 5, DOTA complexes of trivalent metals such as Sc or In were bound with much lower affinities (<1% Y-DOTA).

5.7. Copper-64 and -67

Copper has two oxidation states of importance to radiopharmaceuticals: Cu(I) and Cu(II), with the latter being more prevalent. Kinetic inertness is more important for Cu than thermodynamic stability. Copper has been shown to have

greater kinetic inertness and *in vivo* stability when complexed with macrocyclic chelators than with linear polyamino carboxylates. A number of Cu compounds result in a reduction of Cu(II) to Cu(I) *in vivo* and subsequent loss of the Cu, which can then be complexed by proteins such as superoxide dismutase (SOD) and result in accumulation of Cu in the liver.⁸⁴ Copper forms compounds with coordination numbers ranging from four to six and prefers binding to nitrogen-containing functional groups.

There are two major radionuclides of Cu that are of interest for theranostic applications: ⁶⁴Cu and ⁶⁷Cu. Copper-67 with a half-life of 2.58 days emits a maximum energy β^- particle of 0.577 MeV. It is produced on a high-energy accelerator by bombarding an enriched ⁶⁸Zn target with 193 MeV high-energy protons by the nuclear reaction ⁶⁸Zn(p,2p)⁶⁷Cu. It can also be produced in a reactor by irradiation of enriched ⁶⁷Zn oxide by the nuclear reaction ⁶⁷Zn(n,p)⁶⁷Cu. This reaction, however, is low yielding and results in the production of ⁶⁵Zn, a long-lived radionuclide resulting in expensive waste disposal. The targets are processed as previously described.⁶⁷ Briefly, the targets are dissolved in concentrated HCl, the Cu is selectively removed using Chelex, and a final purification is performed with an anion exchange column to remove impurities such as Ga, Fe, and Co. The Cu is eluted in a high concentration of acid, dried down, and reconstituted in dilute HCl.

Although there is significant interest in ⁶⁷Cu, its use is curtailed by its low availability. Currently production is limited to only a few sites worldwide that make approximately 100 mCi per month. Another copper isotope, ⁶²Cu (half-life = 9.7 min, β^+ 2.9 MeV (97%), EC 2%), can be obtained from a ⁶²Zn/⁶²Cu generator. The 9.3 h half-life of the ⁶²Zn parent is compatible with centralized generator production and delivery to clinical sites. ⁶²Cu can be eluted from the ⁶²Zn/⁶²Cu generator every 30 min over an 8 h period. Three other radionuclides of Cu can be made on medium energy cyclotrons: ⁶⁰Cu with a half-life of 15 min, ⁶¹Cu with a half-life of 3.3 h, and ⁶⁴Cu with a half-life of 12.7 h. All are produced by proton irradiation of an enriched nickel target following the nuclear reaction listed for ⁶⁴Cu, ⁶⁴Ni(p,n)⁶⁴Cu. The target and radiometal are dissolved in acid and separated on an anion exchange column using various acid concentrations to selectively elute the different metals and remove impurities. The Cu is then dried down and reconstituted in dilute HCl. A number of institutions are currently supplying ⁶⁴Cu on a routine basis. Copper-64 decays 19% by positron emission (0.653 MeV), 40% by β^- emission (0.579 MeV), and 41% by electron capture and can be used for both imaging and therapeutic applications. In addition to its use in radiopharmaceuticals as ⁶⁴Cu, elemental Cu has been used to study various diseases involving Cu metabolism including Menke's⁸⁵ and Wilson's⁸⁶ diseases.

Radiopharmaceuticals labeled with a variety of copper radionuclides have been developed for several applications. These radiopharmaceuticals can be grouped into two general categories: specifically designed small molecules, and biological vehicles for selective targeting such as radiolabeled peptides and antibodies. Copper-labeled PTSM (pyruvaldehyde-bis-(N⁴-methylthiosemicarbazone), Figure 2)⁸⁷ is an agent that can be used to measure blood flow in the heart⁸⁸ and brain.⁸⁹ The mechanism of uptake has been proposed⁹⁰ to result from the reductive decomposition of the Cu(II) complex by intracellular sulfhydryls (such as glutathione) resulting in the loss and trapping of Cu(II) in the tissue. Cu-ATSM (diacetyl-bis(N⁴-methylthiosemicarbazone), Figure 2), an analog in which a

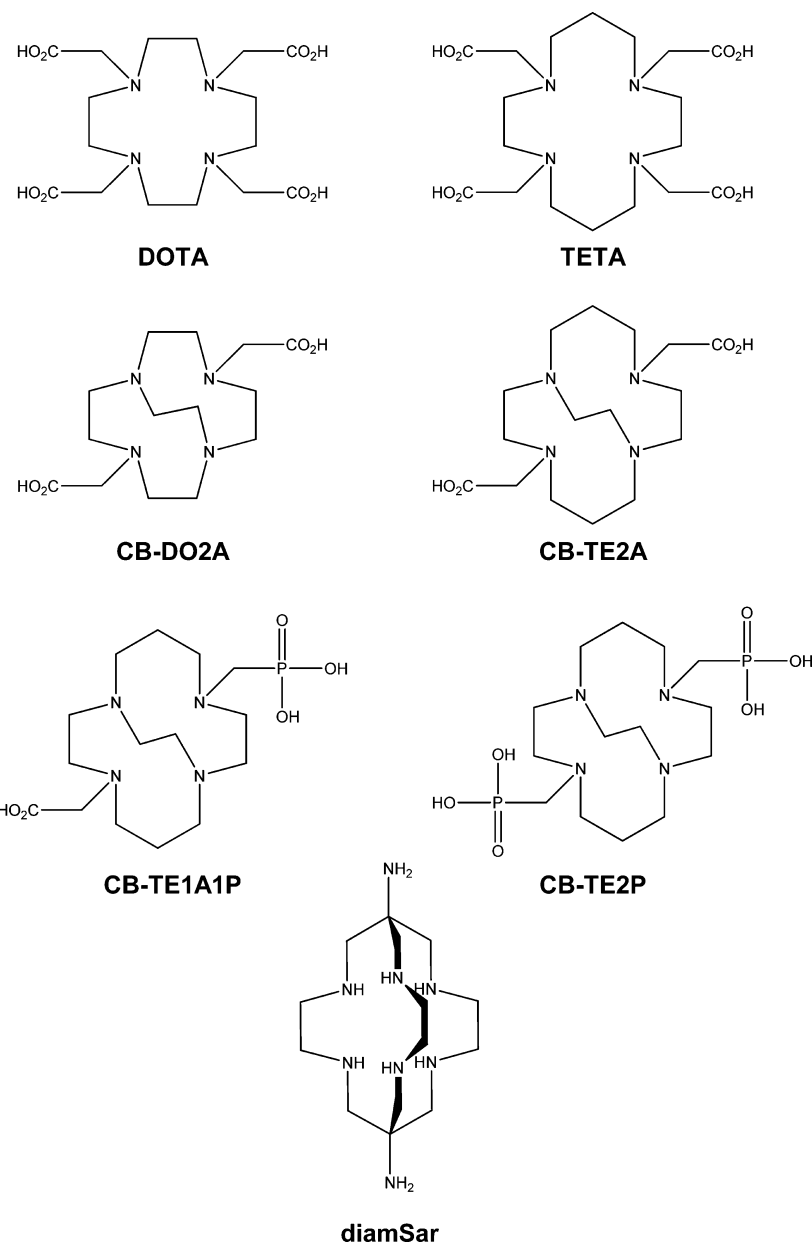


Figure 12. Structures of Cu ligands: DOTA, TETA, CB-DO2A, CB-TE2A, CB-TE1A1P, CB-TE2P, and diamSAR.

methyl group has been added to the backbone, is used to image hypoxic tissue present in tumors and cardiac tissue. The Cu(II) is reduced to Cu(I) in hypoxic tissue and becomes trapped, whereas in normoxic tissue there is no trapping. The presence of hypoxic tissue in tumors is predictive of a low response to treatments that are oxygen dependent. This selective trapping allows for the imaging and diagnosis of hypoxic tissue and thus aids in treatment selection. Clinical trials in cervical, lung, and rectal cancers have shown that a high uptake within an hour postinjection is indicative of a poor treatment response. Several studies have been carried out to understand the mechanism of uptake of Cu-ATSM in hypoxic tissue.⁹¹ Recently, the ATSM analog has been used as a bifunctional chelator to attach Cu radionuclides to peptides. Several other small molecules have been labeled with ^{64}Cu (Figure 12), for instance, a series of tetraaza macrocyclic ligands with methanephosphonate pendant arms⁹² showing a therapeutic effect on bone tumors or 1,4,7-tris(carboxymethyl)-10-(tetradecyl)-1,4,7,10-tetraazadode-

cane,⁹³ which was shown to be an agent to diagnose Dubin–Johnson Syndrome (DJS).

Another area of research deals with the labeling of peptides and antibodies with Cu radionuclides, which requires the use of bifunctional chelators. A number of the typical chelators have been used, such as EDTA, DTPA, and the common macrocyclic ligands TETA and DOTA shown in Figures 5 and 12. All of these ligands have been shown to be susceptible to the reduction and release of Cu, which is then transchelated to proteins present in both the blood and liver and results in high liver uptake. ^{64}Cu -TETA-Y3-TATE, a somatostatin peptide analog, has been evaluated in a preliminary human study at Washington University in St. Louis.⁹⁴ Compared with ^{111}In -DTPA-octreotide (Octreoscan), more lesions were observed more clearly. Improved ligands have been developed for Cu(II)⁹⁵ such as the cross-bridged chelate CB-TE2A and others shown in Figure 12.⁹⁶ Comparison studies of ^{64}Cu -CB-TE2A-Y3-TATE to ^{64}Cu -TETA-Y3-TATE in AR42J tumor-

bearing rats showed lower blood (4-fold lower at 4 h) and liver (2.4-fold lower) uptake for ^{64}Cu -CB-TE2A-Y3-TATE as well as increased tumor uptake (4.4-fold higher). For some conventional ligands such as TETA or DOTA, it has been shown that some of the copper was released. Other peptides have also been labeled, such as a gastrin releasing peptide,⁹⁷ an arginine-glycine-aspartate (RGD) peptide targeting $\alpha_5\beta_3$ integrin,⁹⁸ and a vasoactive intestinal peptide.⁹⁹ Hexaammine sarcophagine ligands shown in Figure 12 were originally developed by Sargenson. They have been shown to form very stable complexes with Cu(II) with fast labeling kinetics even in dilute concentrations. Due to their high stability and fast labeling they have been modified with a variety of functional groups for attachment to peptides and antibodies. Comparative studies have indicated that the sarcophagine ligands show very high *in vivo* stability and due to their fast labeling conditions are very attractive bifunctional chelators for both diagnostic and therapeutic applications. NOTA analogs have also been evaluated with ^{64}Cu and have demonstrated fast labeling kinetics at low concentrations. Despite the low stability constant of Cu-NOTA of 21.6, NOTA-based ligands have demonstrated high *in vivo* stability with Cu and have resulted in high tumor/liver and tumor/kidney ratios that are some of the best observed for ^{64}Cu .¹⁰⁰ These results are surprising because the stability constant for DTPA with Cu is 21.4, and it demonstrates a much lower stability in the blood compared with NOTA: $14.0\% \pm 12.9\%$ for Cu-DTPA compared with $97\% \pm 3\%$ for Cu-NOTA at 48 h *in vivo*.¹⁰¹ Monoclonal antibodies labeled with ^{64}Cu have been studied both in animal models^{94,102} and in human models,¹⁰³ as well as for human dosimetry.¹⁰⁴ All of these studies have enhanced the use of Cu for potential application in PET imaging. Finally, ^{64}Cu has been used to label nanoparticles¹⁰⁵ that have been shown to be of interest in biomedical applications.^{1,105a}

Copper-67 has long been of interest because of its intermediate energy β^- particles (141 keV average energy), and imageable photons of 184.6 (46.7%), 91.27 (7.3%), and 93.31 (16.6%) keV. Its half-life of 61.83 h is sufficient for the uptake kinetics of many monoclonal antibodies and other carriers administered *in vivo*. It also has easy chemistry for labeling purposes and does not concentrate in sensitive body tissues such as bone marrow. These advantages led to several promising clinical trials that determined MTD and indicated high therapeutic ratios with several tumor regressions. In subsequent clinical studies comparing ^{131}I , ^{90}Y , and ^{67}Cu , therapeutic indices were found to be significantly better for ^{67}Cu , except in the liver. A recent study has evaluated the tissue dosimetry of liposome–radionuclide complexes toward liposome-targeted therapeutic radiopharmaceuticals, notably for ^{67}Cu .¹⁰⁶ They found that ganglioside (GM1) coated-liposomes with ^{67}Cu delivered lower doses to tumor than shorter lived radionuclides such as ^{188}Re and ^{211}At , but ^{67}Cu had a more effective standardized uptake value (SUV).

Copper-67 has been produced by many different routes, both in accelerators and in reactors. However, in the last several decades the only source in the U.S. has been the high-energy proton irradiation of natural zinc targets, irradiated either at the Brookhaven Linac Isotope Producer (BLIP) at Brookhaven National Laboratory, at the Los Alamos Neutron Science Center (LANSCE) at Los Alamos National Laboratory, or at Trace Life Sciences in Denton, TX. It was not possible to provide ^{67}Cu in a time frame suitable to support clinical trials with the attendant schedule fluctuations at the National

Laboratories due to changing patient status. Additionally, the specific activity was at the low end of acceptable for antibody therapy, ranging from 200 to 500 GBq/mg (5.4–13.5 Ci/mg) of ^{67}Cu at the end of bombardment. Another potential source that could be investigated in the U.S. is the $^{70}\text{Zn}(\text{p},\alpha)^{67}\text{Cu}$ reaction, which could contribute small research quantities of up to 0.03 GBq (0.81 mCi) of good specific activity ^{67}Cu . Different routes of production could be pursued that would result in higher yields and possibly the use of linear accelerators. Other routes have been pursued outside of the U.S.

5.8. Arsenic-71, -72, -74, and -77

Arsenic is a member of group 15 of the periodic table and has a Pauling electronegativity of 2.18 and a covalent radius of 1.21 Å. Arsenic has four positron emitting ($^{70/71/72/74}\text{As}$) and three β (negatron) emitting ($^{74/76/77}\text{As}$) radioisotopes with availability from either reactor or accelerator production. The half-lives of these As radioisotopes range from 53 min to 18 days. ^{72}As and ^{77}As are particularly attractive and would both be available in high specific activity, having nuclear properties suitable for PET and radiotherapy, respectively. ^{72}As (half-life 26 h, 88% β^+ , 3.34 MeV) is of interest because it is the daughter of ^{72}Se (8.5 day half-life) and could be available from a generator system provided an efficient Se/As separation method is developed. ^{71}As has a half-life of 64 h and emits a 65.3 MeV positron in 30% abundance. ^{74}As has a half-life of 17.8 days and emits a 426.7 MeV β^+ . ^{77}As (38.8 h half-life, β^- , 0.68 MeV) is available from the decay of ^{77}Ge (11.3 h), which is produced through neutron irradiation of ^{76}Ge . ^{74}As was used in some of the earliest radionuclide imaging studies for the development of PET, at that time, called positrocephalography.¹⁰⁷ Use of arsenic radionuclides has been limited due to availability and issues with separation and purity of the radionuclides. Additionally, few methods are currently available for incorporation of these radionuclides into molecular targeting vectors.

Roesch and Jennewein have developed methods for separation of As from the Ge target that leave the As as the triiodide, a form that can be attached through sulfur coordination to antibodies.¹⁰⁸ This method has been used to label antibodies such as a chimeric IgG₃ antibody ch3g4 and rituximab in high yield and was shown to both maintain the affinity of the antibody and result in high stability out to 72 h.^{108,109}

5.9. Lead-212

Lead is a member of group 14 of the periodic table and has a covalent radius of 1.44 Å and an electronegativity of 1.8 eV. Lead-212 (^{212}Pb) is produced by the decay chain of ^{228}Th and can be obtained from a generator of ^{224}Ac . ^{212}Pb can be used as an *in situ* generator of ^{212}Bi .¹¹⁰ The destruction of radioimmunoconjugate molecules by Auger electrons and electron capture, however, is a major difficulty in radiolabeling a monoclonal antibody with ^{212}Pb . Studies with ^{212}Pb are limited to approaches using an *in vivo* generator as described by Horak et al.,¹¹¹ in which ^{212}Bi is the source of α -particles. The aqueous solution chemistry of Pb(II) complexes was investigated by Pippin et al.¹¹² in the course of developing ^{203}Pb and ^{212}Pb radiolabeled mAbs as imaging agents. The log of the stability constant of the 1:1 Pb–DOTA complex was found to be 24.3, and a biodistribution study suggested that ^{203}Pb –DOTA labeled mAbs were stable *in vivo* and thus useful for tumor localization of Pb(II) radionuclides. A study in mice, however, showed severe bone marrow toxicity with the radiolabeled mAb ^{212}Pb –DOTA–103A, which was responsible for the death of all

animals.¹¹³ Yao et al.¹¹⁴ evaluated the catabolism of mAbs and showed that for internalizing antibodies, CHX-A''-DTPA or DOTA conjugates used for Bi or Pb isotopes, respectively, are adequate and would result in long retention of the tracer in the targeted cells. The internal retention may not be important for short-lived radionuclides such as ²¹³Bi but may be of importance for ²¹²Pb since the decay of ²¹²Pb to its ²¹²Bi daughter results in the release of the ²¹²Bi from the chelate and could possibly be retained intracellularly.

To avoid undesirable radiotoxicity from localization of unchelated ²¹²Bi or ²¹²Pb in natural binding sites, quite stringent requirements are mandated for the complexes: (i) both Pb and Bi should be kinetically inert to dissociation *in vivo*; (ii) the Bi complex should have sufficient thermodynamic stability so that recoil of ²¹²Bi formed from the ²¹²Pb β^- decay does not result in dissociation of the ²¹²Bi; and (iii) the ²¹²Bi complex formed should survive valence shell electronic reorganizations induced by nuclear conversion of the γ rays associated with ²¹²Pb decay. Interpretation of decay effects have been studied for ^{143/144}Ce and ¹⁷⁷Yb.¹¹⁵ Asano et al.¹¹⁶ found that no loss of ¹⁷¹Tb from ¹⁷¹Tb-Cy-DTA was observed from the parent ¹⁷¹Er complex when no free metal was present in solution because a recombination of dissociated metal ion and ligand was possible.

²¹²Pb has been encapsulated into liposomes as demonstrated for Cu, Sc, and Bi. The formation, characterization, stability, and *in vivo* distribution as a function of lipid bilayer membrane was examined by Rosenow et al.¹¹⁷ These authors showed that liposome-associated ²¹²Pb was rapidly taken up in large quantities by the liver and the spleen but liposomes could be stabilized in serum and remained at least partially intact *in vivo*; thus ²¹²Pb liposomes effectively suppressed an antibody response at high doses of activity. The chemical fate of the ²¹²Bi-DOTA complex formed by the β^- decay of ²¹²Pb-(DOTA)²⁻ was examined by Mirzadeh et al.¹¹⁸ who have determined a useful methodology for evaluating the chemical integrity of coordination complexes in such systems.

5.10. Bismuth-212 and -213

Bismuth compounds have been used widely in the clinic for centuries because of their high effectiveness and low toxicities in the treatment of a variety of microbial infections, including syphilis, diarrhea, gastritis, and colitis. The first account of medicinal use was reported in 1786 by Louis Odier for the treatment of dyspepsia. Apart from microbial activity, Bi compounds exhibit anticancer activities; ^{212/213}Bi compounds have also been used as targeted radiotherapeutic agents for cancer treatment, and furthermore they have the ability to reduce the side effects of cisplatin in chemotherapy.

The ^{212/213}Bi radioisotopes are available from generators of ²²⁴Ra and ²²⁵Ac, respectively. Both ^{212/213}Bi decay via branched pathways that result in the emission of both α and β^- particles. Bismuth-213 lacks the high abundance, high energy, and potentially hazardous photon emission of ²¹²Bi and thus is a more attractive candidate for RIT.

Bismuth-212 may be obtained from the decay chain of ²²⁸Th. It decays via a branched pathway by α and β^- emissions to stable ²⁰⁸Pb. However, the short physical half-life of ²¹²Bi may be a problem in terms of the time required for radioimmunoconjugate labeling process and the duration of the access to the tumor. This problem was partially offset by the construction of generators of ²²⁴Ra for the production of ²¹²Bi.

The 3.66 day half-life of ²²⁴Ra could circumvent the short half-life of ²¹²Bi by creating an *in vivo* generator.

The ²¹³Bi decays via a branched pathway by α and β^- emissions to stable ²⁰⁹Bi with 90.3% occurring by α -particle emission (major energy of 8.376 MeV). The 440 keV (27.3%) γ emission allows imaging of tumor uptake and may be used to derive dosimetry. Bismuth-213 is produced from the decay of ²²⁵Ac. A generator has been developed for clinical use¹¹⁹ and has been described elsewhere.^{119a}

Bismuth forms stable complexes with aminopolycarboxylate (APC) and polyaminopolycarboxylate (PAPC) ligands. According to Pearson's hard and soft acid-base theory, Bi(III) is a borderline metal ion, but it has a high affinity for multidentate ligands containing O and N donor atoms.¹²⁰ The chemistry and the structure of Bi(III) complexes with APC and PAPC ligands were reviewed by Stavila et al.¹²¹ and the main characteristics are summarized. The stability constants of Bi(III) complexes of APC and PAPC are usually very high, even at low pH: EDTA-Bi, $\log K_{ML} = 26.7$ (0.5); DOTA-Bi, $\log K_{ML} = 30.3$ (0.5); DTPA-Bi, $\log K_{ML} = 30.7$ (0.5).

Although Bi(III) has a strong tendency to hydrolyze, it is stabilized up to pH 10 in the presence of these strongly chelating ligands. Increasing the number of donor atoms of the ligands and the number of chelating rings formed usually results in higher stability of the complexes. Denticity of the ligands is one of the factors determining the stability of the complexes but also the charge of the ligand, the preorganization, the steric efficiency in which the ligand surrounds the Bi(III) ion to form a cage-like structure. The larger Bi(III) ion (1.03 Å for six coordinate and 1.18 Å for eight coordinate) forms 1:1 or 1:2 complexes with APC and PAPC ligands and exhibits coordination numbers between 7 and 10 with octa-coordination by far the most frequent. Hassfjell and Brechbiel¹²² provided some data concerning the chelation of some PAPC ligands as carrier molecules for ^{212/213}Bi in cancer therapy.

A review of the Bi interactions with potential targeting molecules, including peptides, proteins, and enzymes was published in 2007 by Yang and Sun.¹²³ To direct Bi to the site of disease, a chelating ligand such as DOTA or DTPA is commonly used and forms stable complexes with the radiometal.¹²⁴

The conjugate of ²¹³Bi-CHX-A''-DTPA complex with a humanized anti-CD33 antibody HuM195, an anti-CD45 mAb, and anti-prostate-specific membrane antibody (J591) has been used in preclinical models of leukemia and prostate cancer.¹²⁵ Bismuth-213-labeled HuM195 was entered in a phase I/II clinical trial for advanced myeloid leukemia.¹²⁶ A 2005 review on cancer RIT with α -emitting radionuclides¹²⁷ described in detail all the preclinical *in vitro* and animal studies that have been performed with ²¹²Bi and ²¹³Bi. For ²¹³Bi, human studies were performed that demonstrated specific and potent cell killing ability against leukemia with no significant toxicity¹²⁸ and showed that targeted α particle therapy is feasible in humans.^{125b} Bismuth-213-C595 can inhibit growth of pancreatic cell clusters and preangiogenic lesions *in vivo*, indicating that ²¹³Bi treatment may have a role as adjuvant therapy to prevent early disease recurrence.¹²⁹

Kozak et al.¹³⁰ were the first to demonstrate that ²¹²Bi could be bound to mAb (anti-TAc directed to human interleukin 2 IL-2 receptor) conjugated via a bifunctional metal ligand DTPA. The stability of ²¹²Bi-DTPA-mAb has been demonstrated in an animal model of erythroid leukemia¹³¹ as well as in another leukemia model.¹³² A study on a murine model of

human colon carcinoma (LS174T) was performed¹³³ showing significant antitumoral effects. With mice bearing a human ovarian tumor (SK-OV-3), Horak et al.¹¹¹ proposed a nanogenerator approach (mAb AE1 anti-HER2/neu radiolabeled via bifunctional p-SCN-Bz-DOTA) in which it was shown that a prolongation of survival was obtained while no toxic effect was observed. Bismuth-213-DOTA–biotin conjugates in tumors have been shown to lead to complete tumor elimination in some mice.¹³⁴ A ²¹³Bi-DOTATOC somatostatin analog was evaluated in a preclinical animal model study¹³⁵ and showed significant decrease in tumor growth with minimal organ toxicity (hematologic toxicity). The efficiency of the same ²¹³Bi-DOTATOC was compared with ¹⁷⁷Lu-DOTATOC in human pancreatic adenocarcinoma cells, and results indicated that ²¹³Bi-DOTATOC was therapeutically more effective in increasing survival than ¹⁷⁷Lu-DOTATOC.¹³⁶

Finally, another approach has been developed for the *in vivo* generator ²²⁵Ac/²¹³Bi that could be considered a promising therapeutic agent for disseminated metastatic cancer. Liposomes with encapsulated ²²⁵Ac could be formulated to retain the potentially toxic daughters at the tumor site. Sofou et al.¹³⁷ have developed a passive encapsulation of ²²⁵Ac and tested the retention of ²²⁵Ac and its daughters by stable pegylated phosphatidylcholine cholesterol liposomes of different sizes and charge. These authors showed that multiple ²²⁵Ac could be entrapped per liposome, but because of the size of the liposomal structures required to contain the daughters, the approach is ideally suited for locoregional therapy.

5.11. Tin-117m

Tin is also an element of group 14 of the periodic table and has a covalent radius of 1.40 Å and a Pauling electronegativity of 1.96. Bone pain is a common symptom in disseminated malignancy and may be difficult to manage effectively.¹³⁸ Both ⁸⁹Sr and ³²P were investigated as early as the 1940s for the treatment of metastatic cancer to bone,¹³⁹ and ⁸⁹Sr received FDA approval for routine application in 1993.¹⁴⁰ Radiation is of proven benefit for pain palliation, and there is a growing interest in the therapeutic potential of bone-seeking radiopharmaceuticals. Such palliative treatment of patients with advanced metastatic disease of the skeleton can improve their quality of life dramatically and thus is an important application with many advantages over traditional analgesics and external radiation. The choice of suitable therapeutic radionuclides is limited to the medium energy β^- emitters. Most radioisotopes used for bone pain palliation are reactor-produced.¹⁴¹ Key examples are ¹⁸⁶Re and ¹⁵³Sm, in addition to generator systems that provide a therapeutic daughter from the decay of the parent isotope, such as ¹⁸⁸Re. Tin-117m is another reactor-produced radioisotope, and in contrast to β^- emitters, it emits low-energy conversion electrons that deposit their intense energies (127, 129, and 152 keV) within a short range (0.22–0.29 mm), which can destroy tumors but not damage the bone marrow or other tissues. The 159 keV γ photons are ideal for imaging to monitor cancer.

Tin-117m is produced with relatively low specific activity (74–111 MBq; 2–3 mCi/mg) by neutron irradiation of enriched ¹¹⁶Sn, which can be increased by a factor of 3 by the ¹¹⁷Sn(n,n')^{117m}Sn inelastic route.¹⁴² A method has been investigated for making ^{117m}Sn at an accelerator by the nuclear reaction ¹¹⁶Cd(α ,3n)^{117m}Sn. This requires a 35 MeV α beam, and production yields of 37.5 kBq/(μ A h) for a 13.16 mg/cm² natural cadmium oxide target and 410 kBq/(μ A h) for 11.07 mg/cm² 95% enriched target were obtained. The ^{117m}Sn was

separated from the target by anion exchange achieving a 98% radiochemical yield and 99% radiochemical purity.¹⁴³

Among reactor-produced radioisotopes, Sn has natural affinity for bone, as does Sr. Others such as Sm, Re, and P form stable complexes with bone-seeking carriers such as phosphate and disphosphonate.¹⁴⁴ Bone targeting relies on the principles of selective uptake and prolonged radiopharmaceutical retention at sites of increased bone mineral turnover. Among these, ^{117m}Sn could be considered as a promising radionuclide for therapeutic applications. Of the radiopharmaceuticals examined to date, ^{117m}Sn-DTPA offers the best blood and soft tissue clearance and selective bone uptake.¹⁴⁵ A dose-escalation study reported by Atkins et al.¹⁴⁶ in 1993 demonstrated symptom benefit in 9 of 10 patients treated using 66–573 MBq (1.7–15.5 mCi) ^{117m}Sn-DTPA. Biokinetics and imaging characteristics of ^{117m}Sn-(4+)-DTPA were thus studied by Krishnamurthy et al. in 1997¹⁴⁷ with doses ranging from 8 to 10 MBq/kg (0.2–0.27 mCi/kg). These authors showed that the average biological clearance half-life was 1.45 days for the soft tissue components with 22.4% of the dose; 77.6% of the dose remained on the bone. It was shown that ^{117m}Sn-DTPA behaves similarly to ^{99m}Tc-MDP.

The use of ³²P-phosphate, ⁸⁹Sr, ¹⁵³Sm-EDTMP, ¹⁸⁶Re-HEDP, and ^{117m}Sn-DTPA was reviewed by Lewington¹⁴⁴ in the context of pathophysiology of metastatic bone pain. A comparison of ⁸⁹Sr-chloride, ¹⁵³Sm-EDTMP, ³²P, ¹⁸⁸Re-HEDP, and ^{117m}Sn-DTPA was made by Srivastava.¹⁴⁰ While only limited clinical trials were cited, ^{117m}Sn offers very favorable characteristics. The initial dose is higher than that obtained by ⁸⁹Sr, and *in vitro* and *in vivo* stabilities are very high. Animals studies^{145a} have demonstrated that the stannic form of ^{117m}Sn-DTPA behaved much differently from the stannous form. The clearance rate from blood was considerably slower than other bone agents and urinary excretion was also slower. However, this slow clearance was not problematic; once localized in bone, the ^{117m}Sn remained fixed with no or extremely slow release other than through physical decay.¹⁴⁶ Approximately 70% of the dose was taken up by bone, but this was highly variable and dependent on the extent of disease. Extended phase II and phase III trials were under consideration for ^{117m}Sn-(stannic) DTPA to demonstrate its lower toxicity compared with other agents such as ⁸⁹Sr or ¹⁵³Sm.¹⁴⁰ In 2004, a report on Radiopharmaceuticals for the Palliation of Painful Bone Metastases pointed out that one phase I trial was performed on ^{117m}Sn-DTPA but showed insufficient evidence to recommend this agent.

The only clinical examples to-date for treating synovial inflammation using a low-energy β -emitter is the use of ¹⁶⁹Er colloids to treat inflammation in the small finger joints.¹⁴⁸ The use of appropriately size particles labeled with ^{117m}Sn was called for by Srivastava in 2002¹⁴⁰ as agents of choice for radiation synovectomy.

5.12. Gallium-67 and Indium-111

Gallium and indium are both elements of group 13 of the periodic table with gallium having a radius of 1.13 Å and the larger indium with a radius of 1.32 Å. The Pauling electronegativity of Ga is 1.81 and that for In is 1.78. Gallium-67 and indium-111 have normally been used in nuclear medicine for SPECT imaging and, due to their conversion and Auger electrons, are being considered for therapeutic applications as well. Gallium-67 has a half-life of 3.26 days and decays 100% by electron capture. Indium-111 has

a half-life of 2.8 days and decays by electron capture with emission of γ rays of 173 and 247 keV (89% and 95% abundance, respectively). Although they can form different oxidation states the only one of relevance for radiopharmaceuticals is the +3 oxidation state. Gallium and In are classified as hard metals that tend to bind to harder oxygen donor containing ligands and also sulfur- and nitrogen-containing ligands. Gallium differs from indium in that it hydrolyzes at pH greater than 3, so most labeling is done between pH 3 and 4 for Ga complexes. Gallium(III) forms stable four, five, and six coordinate complexes, with six being the most stable. Indium, with its slightly larger ionic radius, forms complexes with coordination numbers of four through seven, with six being the most stable.

Gallium in particular is very similar to Fe(III), having a similar ionization potential and ionic radius with Fe(III) having a half-filled 3d orbital and Ga(III) a filled 3d orbital. A consequence of this is that Ga(III) readily binds to iron-containing proteins, particularly transferrin. This has been used to image inflammation and tumors by injection of ^{68}Ga bound to the weak chelator, citrate, that upon injection releases ^{68}Ga , which then transchelates to transferrin and is taken up through the transferrin receptor. Thus, thermodynamic stability is a strong predictor of *in vivo* stability for Ga and In complexes and needs to be above that of the transferrin formation constant, which is 20.3 for Ga and 18.4 for In. Most reactions with Ga and In require the use of exchange ligands to keep the metal hydroxides from forming before the metal binds with the ligands.

Gallium-67 is typically produced on a cyclotron by proton irradiation on an isotopically enriched ^{68}Zn target by the nuclear reaction $^{68}\text{Zn}(\text{p},2\text{n})^{67}\text{Ga}$.

The most common separation techniques utilize solvent extraction, ion exchange, or a combination of both to separate the ^{67}Ga from the zinc target material. Indium-111 is also produced on a high-energy cyclotron by proton bombardment of an enriched ^{111}Cd target. The ^{111}In thus produced is separated from the Cd target by ion exchange, solvent extraction, and precipitation with Fe(OH)_3 .

Biological targeting agents (e.g., receptor seeking moieties) have been labeled with diagnostic radionuclides (e.g., $^{99\text{m}}\text{Tc}$ and ^{111}In) and used successfully to image tumors. Somatostatin is a peptide involved in the regulation and release of certain hormones, including growth hormone, thyroid-stimulating hormone, and prolactin. Many human tumors such as small cell lung, pancreatic, breast, prostate, melanoma, hepatic, and lymphoma are somatostatin receptor positive. The very short biological half-life of native somatostatin (<3 min) precludes its use as a targeting molecule, but analogs such as octreotide have been designed with much longer *in vivo* residence times.²⁵ Radiolabeling octreotide with imaging radioisotopes has allowed successful imaging of somatostatin receptor-positive tumors. For example, ^{111}In -DTPA-octreotide (DTPA = diethylenetriaminepentaacetic acid) is marketed as Octreoscan for imaging and diagnosing somatostatin receptor positive tumors.¹⁴⁹

In addition to imaging, high doses (18.5 GBq; 500 mCi) of Octreoscan have been given to patients with progressive disseminated neuroendocrine tumors. A clinical response was achieved in 84% of the patients with a median survival of 13 months. These patients presented no kidney toxicity, though a grade II liver toxicity was observed in one patient.¹⁵⁰ The results indicated that the treatments were safe and effective;

however the survival rates appeared to be less than those observed for ^{90}Y and ^{177}Lu therapies in similar patients. These studies indicate how Auger electrons can be safely used and how they may change the organ of toxicity, which may be critical for a certain patient population.

6. SUMMARY

Radiometals, due to their diversity in nuclear properties, are expected to see increased application with the growing utilization of both diagnostic and therapeutic radiopharmaceuticals. Due to the large variability observed in patients in the clinic and the need to personalize each patient's diagnosis and treatment, the need for radiometals will grow. By using imaging to assess pharmacokinetics, clearance, dosimetry, and the dose limiting critical organ, it is possible to provide an optimized dose that gives the patient the most effective treatment. In the future, we can expect to see that patients will need agents to assess how their disease is progressing, determine what treatment to use and in what quantities, and assess the effectiveness of their treatment. This will require development of improved production methods to minimize contaminants, improve production yields, and increase radiolabeling yields. Novel methods of radiometal attachment will need to be developed as we continue down the path of personalized medicine. It can be envisioned that specialized drugs will be more and more patient specific and will require the ability to perform tandem and combination treatments, in which more than one radiometal may be required. This will require innovative methods for providing such personalized medicine to improve the survival and quality of life of each patient.

AUTHOR INFORMATION

Notes

The authors declare no competing financial interest.

Biographies



Cathy S. Cutler obtained her B.S. in Biochemistry in 1988 and her Ph.D. in Inorganic chemistry in 1993 at the University of Cincinnati under the guidance of Professor Deutsch. Subsequently, she worked as a postdoctorate fellow and group manager under Dr. William R. Heineman studying the *in vivo* mechanism of $^{99\text{m}}\text{Tc}$ -PAO brain agents. In 1998, Dr. Cutler joined the Radiation Sciences group at Washington University in St. Louis under the supervision of Professor Michael J. Welch. She then moved to the MU Research Reactor Center where she is now a Research Professor, a member of the Nuclear Sciences and Engineering Institute, and an Adjunct Professor of Nuclear Engineering. Her research ranges from making use of inorganic chemistry to designing new metal-based radiopharmaceuticals and

evaluating their *in vivo* behavior to developing analytical techniques for the isolation, purification, and characterization of radioisotopes and radiopharmaceuticals. Another focus is developing production and separation methods for no carrier added radioisotopes to create a suite of agents for personalized patient treatments.



Heather M. Hennkens obtained her B.S. in chemistry and B.A. in Spanish at Lindenwood University and her M.A. in inorganic chemistry at Washington University in St. Louis. She earned her Ph.D. in inorganic and radiopharmaceutical chemistry at Washington University in St. Louis in 2004 under the supervision of the late Professor Michael J. Welch. She completed her training with Professors Michael R. Lewis and Silvia S. Jurisson at the University of Missouri (MU), during which she was both a MU Life Sciences and a National Institutes of Health National Research Service Award (NRSA) postdoctoral fellow. After spending 2 years as a bioanalytical Study Director in the pharmaceutical industry at ABC Laboratories, Inc., she resumed her academic career at the MU Research Reactor Center in 2011, where she is an Assistant Research Professor. Her budding research program focuses on the development of radiometal-labeled molecular probes for use as radiopharmaceuticals in PET and SPECT imaging and targeted radiotherapy of disease, primarily cancer.



Nebiat Sisay was born in Addis Ababa, Ethiopia, in 1981. He received his B.S. in chemistry in 2008 from Southern University at New Orleans. During his undergraduate studies, he participated in research programs for two consecutive summers at the University of Missouri where he is now pursuing his graduate degree. He is currently working under the supervision of Silvia S Jurisson and Cathy Cutler in research projects including separation and purification of radiolanthanides and the selection of small peptides with affinity for radioconjugates.



Sandrine Huclier-Markai earned her Ph.D. in radiochemistry and analytical chemistry in 2002 from Nantes University (France) with Prof. B. Grambow. She had a postdoctoral training in a Service of Metrology and Analysis of Radioactivity and Trace elements. She has begun her academic career at University of Toulon (France) in 2003 where she worked on the transfer of metallic contaminants and radionuclides in the ecosystems. She moved back to Nantes University in 2006 where she has been involved in radiopharmaceutical chemistry, radioenvironmental chemistry, and development of original analytical tools. She is actively involved in training students at all levels in general chemistry and radiochemistry research. She is also involved in several International Scientific Committees of international conferences of reference in Radiochemistry.



Silvia S. Jurisson earned her B.S. in Chemistry from the University of Delaware in 1978 and her Ph.D. in inorganic and radiopharmaceutical chemistry at the University of Cincinnati with Professor Ed Deutsch in 1982. She had postdoctoral training at the University of New South Wales with Professor W. Greg Jackson, the Australian National University with Professor Alan M. Sargeson, and the University of Missouri with Professor David E. Troutner. She spent 5 years in the pharmaceutical industry at Squibb/Bristol-Myers-Squibb before beginning her academic career at the University of Missouri in 1991 and where she is now a Professor of Chemistry. She has been involved in inorganic and radiochemistry with applications to radiopharmaceutical chemistry, radioenvironmental chemistry, and biological systems. She is actively involved in training students at all levels in inorganic and radiochemistry research.

REFERENCES

- (1) Rossin, R.; Pan, D.; Qi, K.; Turner, J. L.; Sun, X.; Wooley, K. L.; Welch Michael, J. *J. Nucl. Med.* **2005**, *46*, 1210.
- (2) Coleman, R. E. In *Holland-Frei Cancer Medicine*, 6th ed.; Kufe, D. W., Pollack, R. E., Weichselbaum, R. R., et al., Eds.; BC Decker: Hamilton, ON, 2003.

- (3) Dijkers, E. C.; Oude Munnink, T. H.; Kosterink, A. G.; Brouwers, A. H.; Jager, P. L.; De Jong, M.; van Dongen, G. A.; Schroder, C. P.; Lub-de Hooge, M. N.; de Vries, E. G. *Clin. Pharmacol. Ther.* **2010**, *87*, 586.
- (4) Cutler, C. S.; Smith, C. J.; Ehrhardt, G. J.; Tyler, T. T.; Jurisson, S. S.; Deutsch, E. *Cancer Biother. Radiopharm.* **2000**, *15*, 531.
- (5) (a) Begg, A. C.; Stewart, F. A.; Vens, C. *Nat. Rev. Cancer* **2011**, *11*, 239. (b) Reilly, R. M., Ed. *Monoclonal Antibody and Peptide-Targeted Radiotherapy of Cancer*; Wiley: Hoboken, NJ, 2010.
- (c) Konijnenberg, M. W.; de Jong, M. *Eur. J. Nucl. Med. Mol. Imaging* **2011**, *38* (Suppl 1), S19. (d) Sgouros, G. *Adv. Drug Delivery Rev.* **2008**, *60*, 1402. (e) Sgouros, G.; Frey, E.; Wahl, R.; He, B.; Prideaux, A.; Hobbs, R. *Semin. Nucl. Med.* **2008**, *38*, 321. (f) Brans, B.; Bodei, L.; Giannarini, F.; Linden, O.; Luster, M.; Oyen, W. J. G.; Tennvall, J. *Eur. J. Nucl. Med. Mol. Imaging* **2007**, *34*, 772. (g) Bardies, M.; Buvat, I. *Q. J. Nucl. Med. Mol. Imaging* **2011**, *55*, S. (h) Stabin, M. G. *Cancer Biother. Radiopharm.* **2008**, *23*, 273. (i) Wierts, R.; de Pont, C. D. J. M.; Brans, B.; Mottaghay, F. M.; Kemerink, G. J. *Methods* **2011**, *55*, 196.
- (6) Srivastava, S. C. *Semin. Nucl. Med.* **2012**, *42*, 151.
- (7) Baum, R. P.; Kulkarni, H. R.; Carreras, C. *Semin. Nucl. Med.* **2012**, *42*, 190.
- (8) Barnholtz, S. L.; Lydon, J. D.; Huang, G.; Venkatesh, M.; Barnes, C. L.; Ketrin, A. R.; Jurisson, S. S. *Inorg. Chem.* **2001**, *40*, 972.
- (9) Berning, D. E.; Katti, K. V.; Barnes, C. L.; Volkert, W. A. *Chem. Ber./Recl.* **1997**, *130*, 907.
- (10) Berning, D. E.; Katti, K. V.; Volkert, W. A.; Higginbotham, C. J.; Ketrin, A. R. *Nucl. Med. Biol.* **1998**, *25*, 577.
- (11) Bottenus, B. N.; Kan, P.; Jenkins, T.; Ballard, B.; Rold, T. L.; Barnes, C.; Cutler, C.; Hoffman, T. J.; Green, M. A.; Jurisson, S. S. *Nucl. Med. Biol.* **2010**, *37*, 41.
- (12) (a) Chanda, N.; Kan, P.; Watkinson, L. D.; Shukla, R.; Zambre, A.; Carmack, T. L.; Engelbrecht, H.; Lever, J. R.; Katti, K.; Fent, G. M.; Casteel, S. W.; Smith, C. J.; Miller, W. H.; Jurisson, S.; Boote, E.; Robertson, J. D.; Cutler, C.; Dobrovolskaia, M.; Kannan, R.; Katti, K. V. *Nanomedicine (Philadelphia, PA, U. S.)* **2010**, *6*, 201. (b) Khan, M. K.; Minc, L. D.; Nigavekar, S. S.; Kariapper, M. S. T.; Nair, B. M.; Schipper, M.; Cook, A. C.; Lesniak, W. G.; Balogh, L. P. *Nanomedicine (N. Y., NY, U. S.)* **2008**, *4*, 57.
- (13) Kannan, R.; Rahing, V.; Cutler, C.; Pandrapragada, R.; Katti, K. K.; Kattumuri, V.; Robertson, J. D.; Casteel, S. J.; Jurisson, S.; Smith, C.; Boote, E.; Katti, K. V. *J. Am. Chem. Soc.* **2006**, *128*, 11342.
- (14) Khan, M. K.; Minc, L. D.; Nigavekar, S. S.; Kariapper, M. S. T.; Nair, B. M.; Schipper, M.; Cook, A. C.; Lesniak, W. G.; Balogh, L. P. *Nanomedicine* **2008**, *4*, 57.
- (15) Shukla, R.; Chanda, N.; Zambre, A.; Upendran, A.; Katti, K.; Kulkarni, R. R.; Nune, S. K.; Casteel, S. W.; Smith, C. J.; Vimal, J.; Boote, E.; Robertson, J. D.; Kan, P.; Engelbrecht, H.; Watkinson, L. D.; Carmack, T. L.; Lever, J. R.; Cutler, C. S.; Caldwell, C.; Kannan, R.; Katti, K. V. *Proc. Natl. Acad. Sci. U.S.A.* **2012**, *109*, 12426; DOI: 10.1073/pnas.1121174109.
- (16) Tachibana, H.; Koga, K.; Fujimura, Y.; Yamada, K. *Nat. Struct. Mol. Biol.* **2004**, *11*, 380.
- (17) Shukla, R.; Chanda, N.; Zambre, A.; Upendran, A.; Katti, K.; Kulkarni, R. R.; Nune, S. K.; Casteel, S. W.; Smith, C. J.; Vimal, J.; Boote, E.; Robertson, J. D.; Kan, P.; Engelbrecht, H.; Watkinson, L. D.; Carmack, T. L.; Lever, J. R.; Cutler, C. S.; Caldwell, C.; Kannan, R.; Katti, K. V. *Proc. Natl. Acad. Sci. U.S.A.* **2012**, *109*, 12426.
- (18) McLaughlin, M.; Chanda, N.; Lever, J. R.; Smith, C. J.; Kannan, R.; Katti, K. V.; Katti, K.; Cutler, C. S. *J. Labelled Compd. Radiopharm.* **2011**, *54*, S549.
- (19) Smith, C. J.; Volkert, W. A.; Hoffman, T. J. *Nucl. Med. Biol.* **2003**, *30*, 861.
- (20) McLaughlin, M.; Chanda, N.; Lever, J. R.; Smith, C. J.; Kannan, R.; Katti, K.; Katti, K.; Cutler, C. S. *J. Labelled Compd. Radiopharm.* **2011**, *54*, S549.
- (21) (a) Hainfeld, J. F. *Science* **1987**, *236*, 450. (b) Anderson, P.; Vaughan, A. T. M.; Varley, N. R. *Nucl. Med. Biol.* **1988**, *15*, 293. (c) Hainfeld, J. F. *Nature* **1988**, *333*, 281. (d) Hainfeld, J. F.; Foley, C. J.; Srivastava, S. C.; Mausner, L. F.; Feng, N. I.; Meinken, G. E.; Steplewski, Z. *Int. J. Radiat. Appl. Instrum. B* **1990**, *17*, 287. (e) Kolsky, K. L.; Mausner, L. F. *Appl. Radiat. Isot.* **1993**, *44*, 553. (f) Kolsky, K. L.; Joshi, V.; Mausner, L. F.; Srivastava, S. C. *Appl. Radiat. Isot.* **1998**, *49*, 1541.
- (22) Grazman, B.; Troutner, D. E. *Appl. Radiat. Isot.* **1988**, *39*, 257.
- (23) Jia, W.; Ma, D.; Volkert, E. W.; Ketrin, A. R.; Ehrhardt, G. J.; Jurisson, S. S. *Platinum Met. Rev.* **2000**, *44*, 50.
- (24) Efe, G. E.; Pillai, M. R. A.; Schlemper, E. O.; Troutner, D. E. *Polyhedron* **1991**, *10*, 1617.
- (25) Pillai, M. R. A.; John, C. S.; Troutner, D. E. *Bioconjugate Chem.* **1990**, *1*, 191.
- (26) Pillai, M. R. A.; Lo, J. M.; Troutner, D. E. *Appl. Radiat. Isot.* **1990**, *41*, 69.
- (27) Venkatesh, M.; Goswami, N.; Volkert, W. A.; Schlemper, E. O.; Ketrin, A. R.; Barnes, C. L.; Jurisson, S. S. *Nucl. Med. Biol.* **1996**, *23*, 33.
- (28) (a) Goswami, N. A.; Alberto, R.; Barnes, C. L.; Jurisson, S. S. *Inorg. Chem.* **1996**, *35*, 7546. (b) Goswami, N.; Higginbotham, C.; Volkert, W. A.; Alberto, R.; Nef, W.; Jurisson, S. S. *Nucl. Med. Biol.* **1999**, *26*, 951.
- (29) (a) Li, N.; Eberlein, C. M.; Volkert, W. A.; Ochrymowycz, L.; Barnes, C. L.; Ketrin, A. R. *Radiochim. Acta* **1996**, *75*, 83. (b) Li, N.; Struttman, M.; Higginbotham, C.; Grall, A. J.; Skerlj, J. F.; Vollano, J. F.; Bridger, S. A.; Ochrymowycz, L. A.; Ketrin, A. R.; Abrams, M. J.; Volkert, W. A. *Nucl. Med. Biol.* **1997**, *24*, 85.
- (30) Goodman, D. C.; Reibenspies, J. H.; Goswami, N.; Jurisson, S. S.; Darenbourg, M. Y. *J. Am. Chem. Soc.* **1997**, *119*, 4955.
- (31) Akgun, Z.; Engelbrecht, H.; Fan, K.-H.; Barnes, C. L.; Cutler, C. S.; Jurisson, S. S.; Lever, S. Z. *Dalton Trans.* **2010**, *39*, 10169.
- (32) (a) Gillard, R. D.; Wilkenson, G. J. *Chem. Soc.* **1964**, 1224. (b) Rund, J. V.; Basalo, F.; Pearson, R. G. *Inorg. Chem.* **1964**, *3*, 658. (c) Addison, A. W.; Gillard, R. D.; Vaughan, H. *J. Chem. Soc., Dalton Trans.* **1973**, 1187–1193.
- (33) Cagnoli, A.; Ballard, B.; Engelbrecht, H.; Rold, T. L.; Kannan, R.; Barnes, C. L.; Cutler, C. S.; Ketrin, A. R.; Katti, K. V.; Jurisson, S. S. *Nucl. Med. Biol.* **2011**, *38*, 63.
- (34) (a) Jurisson Silvia, S.; Berning, D. E.; Jia, W.; Ma, D. *Chem. Rev.* **1993**, *93*, 1137. (b) Jia, W.; Ma, D.; Volkert, E. W.; Ketrin, A. R.; Ehrhardt, G. J.; Jurisson Silvia, S. *Platinum Met. Rev.* **2000**, *44*, 50. (c) Jang, Y. H.; Blanco, M.; Dasgupta, S.; Keire, D. A.; Shively, J. E.; Goddard, W. A., III *J. Am. Chem. Soc.* **1999**, *121*, 6142. (d) Li, M.; Meares, C. F. *Bioconjugate Chem.* **1993**, *4*, 275. (e) Lewis, M. R.; Raubitschek, A. A.; Shively, J. E. *Bioconjugate Chem.* **1994**, *4*, 565.
- (35) Bryan, J. N.; Bommarito, D.; Kim, D. Y.; Berent, L. M.; Bryan, M. E.; Lattimer, J. C.; Ketrin, A. R.; Cutler, C. S. *J. Nucl. Med. Technol.* **2009**, *37*, 45.
- (36) (a) Trindade, V.; Paolino, A.; Rodríguez, G.; Coppe, F.; Fernández, M.; Lopez, A.; Mallo, L.; Oliver, P.; Balter, H.; Gaudiano, J. *Alasbinn J.* **2009**, *46*. (b) Trindade, V.; Rodríguez, G.; Cabral, P.; Fernández, M.; Paolino, A.; Gaudiano, J.; Balter, H. *Alasbinn J.* **2009**, *43*.
- (37) (a) Turner, J. H. *Ann. Nucl. Med.* **2012**, *26*, 289. (b) Bander, N. H.; Milowsky, M. I.; Nanus, D. M.; Kostakoglu, L.; Vallabhajosula, S.; Goldsmith, S. J. *J. Clin. Oncol.* **2005**, *23*, 4591.
- (38) Lantry, L. E.; Cappaletti, E.; Maddalena, M. E.; Fox, J. S.; Feng, W.; Chen, J.; Thomas, R.; Eaton, S. M.; Bogdan, N. J.; Arunachalam, T.; Ruebi, J. C.; Raju, N.; Metcalfe, E. C.; Lattuada, L.; Linder, K. E.; Swenson, R. E.; Tweedle, M. E.; Nunn, A. D. *J. Nucl. Med.* **2006**, *47*, 1144.
- (39) Mansi, R.; Wang, X.; Forrer, F.; Waser, B.; Cescato, R.; Graham, K.; Borkowski, S.; Reubi, J. C.; Maecke, H. R. *Eur. J. Nucl. Med. Mol. Imaging* **2011**, *38*, 97.
- (40) Rossin, R.; Verkerk, P. R.; van den Bosch, S. M.; Vulders, R. C. M.; Verel, R.; Lub, J.; Robillard, M. S. *Angew. Chem., Int. Ed.* **2010**, *49*, 3375.
- (41) (a) Murara, R.; Kurakao, M.; Wunderlich, D.; Poole, D. J.; Colcher, D.; Thor, A.; Greiner, J. W.; Simpson, J. F.; Molinola, A.; Noguchi, P.; Shclom, J. *Cancer Res.* **1988**, *48*, 4588. (b) Shclom, J.;

- Eggensberger, D.; Colcher, D.; Molinola, D.; Houchens, L. S.; Miller, L. S.; Hinkle, G.; Siler, K. *Cancer Res.* **1992**, *52*, 1067.
- (42) Rossin, R.; Sandra, M.; van den Bosch, S. M.; Robillard, M. S. Presented at the World Molecular Imaging Congress, San Diego, CA, 2011.
- (43) Eary, J. F.; Collins, C.; Stabin, M.; Vernon, C.; Petersdorf, S.; Baker, M.; Hartnett, S.; Ferency, S.; Addison, S. J.; Appelbaum, F.; Godon, E. E. *J. Nucl. Med.* **1993**, *34*, 1031.
- (44) Turner, J. H.; Claringbold, P. G.; Hetherington, E. L.; Sorby, P.; Martindale, A. A. *J. Clin. Oncol.* **1989**, *7*, 1926–1931.
- (45) Sinzinger, H.; Palumbo, B.; Granegger, S. *J. Nucl. Med.* **2008**, *49* (Suppl.), 369.
- (46) (a) Morris, M. J.; Pandit-Taskar, J.; Carrasquillo, C. R.; Divgi, S.; Slovin, W. K.; Kelly, D.; Rathkopf, G. A.; Gignac, D.; Solit, L.; Schwartz, R. D.; Stephenson, C.; Hong, A.; Delacruz, T.; Curley, G.; Heller, X.; Jia, J.; O'Donoghue, J.; Larson, S.; Scher, H. I. *J. Clin. Oncol.* **2009**, *27*, 2436. (b) Fizazi, K.; Beuzeboc, P.; Lumbroso, J.; Haddad, V.; Massard, C.; Gross-Gouipil, M.; Di Palma, M.; Escudier, B.; Theodore, C.; Loriot, Y.; Tournay, E.; Bouzy, J.; Laplanche, A. *J. Clin. Oncol.* **2009**, *27*, 2429.
- (47) Breitz, H. B.; Wendt, R. E., III; Stabin, M. S.; Shen, S.; Erwin, W. D.; Rajendran, J. G.; Eary, J. F.; Durack, L.; Delpassand, E. S.; Martin, W.; Meredith, R. F. *J. Nucl. Med.* **2006**, *47*, 534.
- (48) Chatterjee, M.; Chakraborty, T.; Tassone, P. *Eur. J. Cancer* **2006**, *42*, 1640.
- (49) de Jong, M.; Breeman, W. A.; Bernard, B. F.; Rolleman, E. J.; Hofand, L. J.; Visser, T. J.; Setyano-Han, B.; Bakker, W. H.; van der Pluijm, M. E.; Krenning, E. P. *Eur. J. Nucl. Med.* **1995**, *22*, 608.
- (50) Lehenberger, S.; Barkhausen, C.; Cohrs, S.; Fischer, E.; Grunberg, J.; Honr, A.; Koster, U.; Shibli, R.; Turler, A.; Zhernosekov, K. *Nucl. Med. Biol.* **2011**, *38*, 917.
- (51) Cutler, C. S.; Cantorius, M. C.; Kelsey, J. C.; Engelbrecht, H. P.; Forbis, L. J.; Embree, M. F.; Wilder, S. L.; Lever, J. R.; Watkinson, L. D.; Carmack, T. L.; Lewis, M. R.; Bigott-Hennkens, H. M.; Dannon, S. J. *Labelled Compd. Radiopharm.* **2009**, *52*, S96.
- (52) (a) W.P., L.; Smith, C. J.; Cutler, C. S.; Hoffman, T. J.; Ketring, A. R.; Jurisson Silvia, S. *Nucl. Med. Biol.* **2003**, *30*, 241. (b) Lewis, M. R.; Zhang, J.; Jia, F.; Owen, N. K.; Cutler, C. S.; Embree, M. F.; Schutlz, J.; Theodore, L. J.; Ketring, A. R.; Jurisson Silvia, S.; Axworthy, D. B. *Nucl. Med. Biol.* **2004**, *31*, 213. (c) Mohsin, H.; Jia, F.; Bryan, J.; Sivaguru, G.; Cutler, C. S.; Ketring, A. R.; Miller, W. H.; Simon, J.; Frank, R. K.; Theodore, L. J.; Axworthy, D. B.; Jurisson, S. S.; Lewis, M. R. *Bioconjugate Chem.* **2011**, *22*, 2444.
- (53) (a) W.P., L.; Ma, D. S.; Higginbotham, C.; Hoffman Timothy, J.; Ketring, A. R.; Cutler, C. S.; Jurisson Silvia, S. *Nucl. Med. Biol.* **2001**, *28*, 145. (b) Stimmel, J. B.; Kull, C. F. *J. Nucl. Med. Biol.* **1998**, *25*, 117.
- (54) (a) Liu, S. *Adv. Drug Delivery Rev.* **2008**, *60*, 1347. (b) Donnelly, P. S. *Dalton Trans.* **2011**, *40*, 999.
- (55) Benny, P. D.; Green, J. L.; Engelbrecht, H. P.; Barnes, C. L.; Jurisson, S. S. *Inorg. Chem.* **2005**, *44*, 2381.
- (56) (a) Lapi, S.; Mills, W. J.; Wilson, J.; McQuarrie, S.; Publicover, J.; Schueler, M.; Schyler, D.; Ressler, J. J.; Ruth, T. J. *Appl. Radiat. Isot.* **2007**, *65*, 345. (b) Szeleczenyi, F.; Steyn, G. F.; Kovacs, Z.; Aardaneh, K.; Vermeulen, C.; Walt, T. N. *J. Radioanal. Nucl. Chem.* **2009**, *282*, 261. (c) Bonardi, M. L.; Groppi, F.; Manenti, S.; Persico, E.; Gini, L.; Abbas, K.; Holzwarth, U.; Simonelli, F.; Alfassi, Z. B. *J. Radioanal. Nucl. Chem.* **2010**, *286*, 1.
- (57) (a) Zuckier, L. S.; Dohan, O.; Li, Y.; Chang, C. J.; Carrasco, N.; Dadachova, E. *J. Nucl. Med.* **2004**, *45*, 500. (b) Haenscheid, H.; Reiners, C.; Goulko, G.; Luster, M.; Schneider-Ludorff, M.; Buck, A. K.; Lassmann, M. *J. Clin. Endocrinol. Metab.* **2011**, *96*, 3511.
- (58) Blower, P. J.; Prakash, S. *Perspect. Bioinorg. Chem.* **1999**, *4*, 91.
- (59) Liu, G.; Hnatowich, D. J. *Anti-Cancer Agents Med. Chem.* **2007**, *7*, 367.
- (60) (a) Francesconi, L. C.; Graczyk, G.; Wehrli, S.; Shaikh, S. N.; McClinton, D.; Liu, S.; Zubietta, J.; Kung, H. F. *Inorg. Chem.* **1993**, *32*, 3114. (b) O'Neil, J. P.; Wilson, S. R.; Katzenellenbogen, J. A. *Inorg. Chem.* **1994**, *33*, 319.
- (61) (a) Giblin, M. F.; Wang, N.; Hoffman, T. J.; Jurisson, S. S.; Quinn, T. P. *Proc. Natl. Acad. Sci. U.S.A.* **1998**, *95*, 12814. (b) Bigott-Hennkens, H. M.; Junnotula, S.; Ma, L.; Gallazzi, F.; Lewis, M. R.; Jurisson, S. S. *J. Med. Chem.* **2008**, *51*, 1223.
- (62) Schibli, R.; Schwarzbach, R.; Alberto, R.; Ortner, K.; Schmalke, H.; Dumas, C.; Egli, A.; Schubiger, P. A. *Bioconjugate Chem.* **2002**, *13*, 750.
- (63) (a) Cheng, A.; Chen, S.; Zhang, Y.; Yin, D.; Dong, M. *Cancer Biother. Radiopharm.* **2011**, *26*, 237. (b) Liepe, K.; Kotzerke, J. *Nucl. Med. Commun.* **2007**, *28*, 623. (c) Paes, F. M.; Serafini, A. N. *Semin. Nucl. Med.* **2010**, *40*, 89.
- (64) Raoul, J.-L.; Boucher, E.; Rolland, Y.; Garin, E. *Nat. Rev. Gastroenterol. Hepatol.* **2010**, *7*, 41.
- (65) Edelman, M. J.; Clamon, G.; Kahn, D.; Magram, M.; Lister-James, J.; Line Bruce, R. *J. Thorac. Oncol.* **2009**, *4*, 1550.
- (66) Klett, R.; Lange, U.; Haas, H.; Voth, M.; Pinkert, J. *Rheumatology (Oxford, U.K.)* **2007**, *46*, 1531.
- (67) Mausner, L. F.; Kolsky, K. L.; Joshi, V.; Srivastava, S. C. *Appl. Radiat. Isot.* **1998**, *49*, 285.
- (68) (a) Roesch, F. *Curr. Radiopharm.* **2012**, *5*, 187. (b) Filosofov, D. V.; Loktionova, N. S.; Rosch, F. *Radiochim. Acta* **2010**, *98*, 149.
- (69) (a) Loncin, M. F.; Desreux, J. F.; Merciny, E. *Inorg. Chem.* **1986**, *25*, 2646. (b) Moi, M. K.; Meares, C. F.; DeNardo, S. J. *J. Am. Chem. Soc.* **1988**, *110*, 6266. (c) Wu, A. M.; Yazaki, P. J.; Tsai, S.-W.; Nguyen, K.; Anderson, A.-L.; McCarthy, D. W.; Welch, M. J.; Shively, J. E.; Williams, L. E.; Raubitschek, A. A.; Wong, J. Y. C.; Toyokuni, T.; Phelps, M. E.; Gambhir, S. S. *Proc. Natl. Acad. Sci. U.S.A.* **2000**, *97*, 8495. (d) Waldherr, C.; Pless, M.; Maecke, H. R.; Schumacher, T.; Cazzolara, A.; Nitzsche, E. U.; Haldemann, A.; Mueller-Brand, J. *J. Nucl. Med.* **2002**, *43*, 610.
- (70) Rosoff, B.; Siegel, E.; Williams, G. L.; Spencer, H. *Int. J. Appl. Radiat. Isot.* **1963**, *14*, 129.
- (71) Benetollo, F.; Bombieri, G.; Calabi, L.; Aime, S.; Botta, M. *Inorg. Chem.* **2003**, *42*, 148.
- (72) Huclier-Markai, S.; Sabatie, A.; Ribet, S.; Kubicek, V.; Paris, M.; Vidaud, C.; Hermann, P.; Cutler, C. S. *Radiochim. Acta* **2011**, *99*, 653.
- (73) (a) Pruszynski, M.; Majkowska-Pilip, A.; Loktionova, N. S.; Eppard, E.; Roesch, F. *Appl. Radiat. Isot.* **2012**, *70*, 974. (b) Koumarianou, E.; Loktionova, N. S.; Fellner, M.; Roesch, F.; Thews, O.; Pawlak, D.; Archimandritis, S. C.; Mikolajczak, R. *Appl. Radiat. Isot.* **2012**, *70*, 2669.
- (74) Ford-Hutchinson, A. W.; Perkins, D. J. *Radiat. Res.* **1972**, *51*, 244.
- (75) Hirano, S.; Suzuki, K. T. *Environ. Health Perspect. Suppl.* **1996**, *104*, 85.
- (76) Rosoff, B.; Spencer, H. *Health Phys.* **1975**, *28*, 611.
- (77) Moeller, T.; Ulrich, W. F. *J. Inorg. Nucl. Chem.* **1956**, *2*, 164.
- (78) Roques, M.; Roscoff, B.; Hart, M.; Williams, G. *Fed. Proc.* **1961**, *20*.
- (79) Spencer, H.; Rosoff, B. *Health Phys.* **1965**, *11*, 1181.
- (80) Byrd, B. L.; Watson, E. E.; Cloutier, R. J.; Hayes, R. L. *Health Phys.* **1975**, *29*, 375.
- (81) Corneillie, T. M.; Whetstone, P. A.; Fisher, A. J.; Meares, C. F. *J. Am. Chem. Soc.* **2003**, *125*, 3436.
- (82) (a) Shannon, R. D. *Acta Crystallogr.* **1976**, *A32*, 751. (b) Meehan, P. R.; Aris, D. R.; Willey, G. R. *Coord. Chem. Rev.* **1999**, *181*, 121.
- (83) Corneillie, T. M.; Fisher, A. J.; Meares, C. F. *J. Am. Chem. Soc.* **2003**, *125*, 15039.
- (84) Bass, L. A.; Wang, M.; Welch Michael, J.; Anderson Carolyn, J. *Bioconjugate Chem.* **2000**, *11*, 527.
- (85) Herd, S. M.; Camakaris, J.; Christofferson, R.; Wookey, P.; Danks, D. M. *Biochem. J.* **1987**, *247*, 341.
- (86) Gunther, K.; Siegemund, R.; Lossner, J.; Kuhn, H. J. *Radiobiol. Radiother. (Berlin)* **1988**, *29*, 226.
- (87) Green, M. A.; Klippenstein, D. L.; Tennison, J. R. *J. Nucl. Med.* **1988**, *29*, 1549.
- (88) (a) Shelton, M. E.; Green, M. A.; Mathias, C. J.; Welch, M. J.; Bergmann, S. R. *J. Nucl. Med.* **1989**, *30*, 1843. (b) Shelton, M. E.;

- Green, M. A.; Mathias, C. J.; Welch, M. J.; Bergmann, S. R. *Circulation* **1990**, *82*, 990.
- (89) (a) Mathias, C. J.; Welch, M. J.; Raichle, M. E.; Mintun, M. A.; Lich, L. L.; McGuire, A. H.; Zinn, K. R.; John, E. K.; Green, M. A. J. *Nucl. Med.* **1990**, *31*, 351. (b) Green, M. A.; Mathias, C. J.; Welch, M. J.; McGuire, A. H.; Perry, D.; Fernandez-Rubio, F.; Perlmutter, J. S.; Raichle, M. E.; Bergmann, S. R. *J. Nucl. Med.* **1990**, *31*, 1989.
- (90) Barnhart-Bott, A.; Green, M. A. *Nucl. Med. Biol.* **1991**, *18*, 865.
- (91) (a) Fujibayashi, Y.; Cutler, C. S.; Anderson, C. J.; McCarthy, D. W.; Jones, L. A.; Sharp, T.; Yonekura, Y.; Welch, M. J. *Nucl. Med. Biol.* **1999**, *26*, 117. (b) Lewis, J. S.; Sharp, T. L.; Laforest, R.; Fujibayashi, Y.; Welch, M. J. *J. Nucl. Med.* **2001**, *42*, 655. (c) Takahashi, N.; Fujibayashi, Y.; Yonekura, Y.; Welch, M. J.; Waki, A.; Tsuchida, T.; Sadato, N.; Sugimoto, K.; Nakano, A.; Lee, J. D.; Itoh, H. *Ann. Nucl. Med.* **2001**, *15*, 293. (d) Dearling, J. L. J.; Lewis, J. S.; Mullen, G. E. D.; Welch, M. J.; Blower, P. J. *JBIC, J. Biol. Inorg. Chem.* **2002**, *7*, 249. (e) Lewis, J. S.; Herrero, P.; Sharp, T. L.; Engelbach, J. A.; Fujibayashi, Y.; Laforest, R.; Kovacs, A.; Gropler, R. J.; Welch, M. J. *J. Nucl. Med.* **2002**, *43*, 1557. (f) Obata, A.; Yoshimoto, M.; Kasamatsu, S.; Naiki, H.; Takamatsu, S.; Kashikura, K.; Furukawa, T.; Lewis, J. S.; Welch, M. J.; Saji, H.; Yonekura, Y.; Fujibayashi, Y. *Nucl. Med. Biol.* **2003**, *30*, 529.
- (92) Sun, X.; Wuest, M.; Kovacs, Z.; Sherry, A. D.; Motekaitis, R.; Wang, Z.; Martell, A. E.; Welch, M. J.; Anderson, C. J. *JBIC, J. Biol. Inorg. Chem.* **2003**, *8*, 217.
- (93) Yoo, J.; Reichert, D. E.; Kim, J.; Anderson, C. J.; Welch, M. J. *Mol. Imaging* **2005**, *4*, 18.
- (94) Anderson, C. J.; Pajean, T. S.; Edwards, W. B.; Sherman, E. L. C.; Rogers, B. E.; Welch, M. J. *J. Nucl. Med.* **1995**, *36*, 2315.
- (95) Lewis, J. S.; Srinivasan, A.; Schmidt, M. A.; Anderson, C. J. *Nucl. Med. Biol.* **1999**, *26*, 267.
- (96) Sprague, J. E.; Peng, Y.; Sun, X.; Weisman, G. R.; Wong, E. H.; Achilefu, S.; Anderson, C. J. *Clin. Cancer Res.* **2004**, *10*, 8674.
- (97) Rogers, B. E.; Bigott, H. M.; McCarthy, D. W.; Della Manna, D.; Kim, J.; Sharp, T. L.; Welch, M. J. *Bioconjugate Chem.* **2003**, *14*, 756.
- (98) Chen, X.; Hou, Y.; Tohme, M.; Park, R.; Khankaldyan, V.; Gonzales-Gomez, I.; Bading, J. R.; Laug, W. E.; Conti, P. S. *J. Nucl. Med.* **2004**, *45*, 1776.
- (99) Thakur, M. L.; Aruva, M. R.; Gariepy, J.; Acton, P.; Rattan, S.; Prasad, S.; Wickstrom, E.; Alavi, A. *J. Nucl. Med.* **2004**, *45*, 1381.
- (100) Dearling, J. L. J.; Voss, S. D.; Dunning, P.; Snay, E.; Fahey, F.; Smith, S. V.; Huston, J. S.; Meares, C. F.; Treves, S. T.; Packard, A. B. *Nucl. Med. Biol.* **2011**, *38*, 29.
- (101) Cooper, M. S.; Ma, M. T.; Sunasse, K.; Shaw, K. P.; Williams, J. P.; Paul, R. L.; Donnelley, P. S.; Blower, P. J. *Bioconjugate Chem* **2012**, *23*, 1029.
- (102) Li, C.; Ke, S.; Wang, W.; (Board of Regents, the University of Texas System, USA) International Patent Application: 2004-US26220 2005019247, 2005.
- (103) (a) Philpott, G. W.; Schwarz, S. W.; Anderson, C. J.; Dehdashti, F.; Connell, J. M.; Zinn, K. R.; Meares, C. F.; Cutler, P. D.; Welch, M. J.; Siegel, B. A. *J. Nucl. Med.* **1995**, *36*, 1818. (b) Anderson, C. J.; Dehdashti, F.; Cutler, P. D.; Schwarz, S. W.; Laforest, R.; Bass, L. A.; Lewis, J. S.; McCarthy, D. W. *J. Nucl. Med.* **2001**, *42*, 213.
- (104) Cutler, P. D.; Schwarz, S. W.; Anderson, C. J.; Connell, J. M.; Welch, M. J.; Philpott, G. W.; Siegel, B. A. *J. Nucl. Med.* **1995**, *36*, 2363.
- (105) (a) Sun, X.; Rossin, R.; Turner, J. L.; Becker, M. L.; Joralemon, M. J.; Welch, M. J.; Wooley, K. L. *Biomacromolecules* **2005**, *6*, 2541. (b) Akiyama, R.; Kobayashi, S. *Chem. Rev.* **2009**, *109*, 594.
- (106) Kostarelos, K.; Emfietzoglou, D. *Anticancer Res.* **2000**, *20*, 3339.
- (107) Whittier, J. R.; Jacobsen, L. E.; Dhrymiotis, A. *J. Nucl. Med.* **1964**, *5*, 134.
- (108) Jennewein, M.; Hermann, A.; Mason, R. P.; Thorpe, P. E.; Rosch, F. *Nucl. Instrum. Methods Phys. Res.* **2006**, *569*, 512.
- (109) Jennewein, M.; Lewis, M. A.; Zhao, D.; Tsyganov, E.; Slavine, N.; He, J.; Watkins, L.; Kodibagkar, V. D.; O'Kelly, S.; Kulkarni, P.; Antich, P. P.; Hermann, A.; Rosch, F.; Mason, R. P.; Thorpe, P. E. *Clin. Cancer Res.* **2008**, *14*, 1377.
- (110) Mausner, L. F.; Straub, R. F.; Srivastava, S. C. *J. Labelled Compd. Radiopharm.* **1989**, *26*, 498.
- (111) Horak, E.; Hartmann, F.; Garmestani, K.; Wu, C.; Brechbiel, M.; Gansow, O. A.; Landolfi, N. F.; Waldmann, T. A. *J. Nucl. Med.* **1997**, *38*, 1944.
- (112) Pippin, C. G.; McMurry, T. J.; Brechbiel, M. W.; McDonald, M.; Lambrecht, R.; Milenic, D.; Roselli, M.; Colcher, D.; Gansow, O. A. *Inorg. Chim. Acta* **1995**, *239*, 43.
- (113) Ruble, G.; Wu, C.; Squire, R. A.; Gansow, O. A.; Strand, M. *Int. J. Radiat. Oncol., Biol., Phys.* **1996**, *34*, 609.
- (114) Yao, Z.; Garmestani, K.; Wong, K. J.; Park, L. S.; Dadachova, E.; Yordanov, A.; Waldmann, T. A.; Eckelman, W. C.; Paik, C. H.; Carrasquillo, J. A. *J. Nucl. Med.* **2001**, *42*, 1538.
- (115) (a) Glentworth, P.; Wright, C. L. *J. Inorg. Nucl. Chem.* **1969**, *31*, 1263. (b) Shiokawa, T.; Kudo, H.; Omori, T. *Bull. Chem. Soc. Jpn.* **1970**, *43*, 2076.
- (116) Asano, T.; Taniguchi, S. *J. Inorg. Nucl. Chem.* **1978**, *40*, 957.
- (117) Rosenow, M. K.; Zucchini, G. L.; Bridwell, P. M.; Stuart, F. P.; Friedman, A. M. *Int. J. Nucl. Med. Biol.* **1983**, *10*, 189.
- (118) Mirzadeh, S.; Kumar, K.; Gansow, O. A. *Radiochim. Acta* **1993**, *60*, 1.
- (119) (a) McDevitt, M. R.; Finn, R. D.; Sgouros, G.; Ma, D.; Scheinberg, D. A. *Appl. Radiat. Isot.* **1999**, *50*, 895. (b) Finn, R.; McDevitt, M.; Scheinberg, D.; Juricic, J.; Larson, S.; Sgouros, G.; Humml, J.; Curciol, M.; Brechbiel, M.; Gansow; Geerlings Sr., M.; Apostolidis, C.; Molinet, R. *J. Labelled Compd. Radiopharm.* **1997**, *40*, 293.
- (120) Briand, G. G.; Burford, N. *Adv. Inorg. Chem.* **2000**, *50*, 285.
- (121) Stavila, V.; Davidovich, R. L.; Gulea, A.; Whitmire, K. H. *Coord. Chem. Rev.* **2006**, *250*, 2782.
- (122) Hassjell, S.; Brechbiel, M. W. *Chem. Rev.* **2001**, *101*, 2019.
- (123) Yang, N.; Sun, H. *Coord. Chem. Rev.* **2007**, *251*, 2354.
- (124) Mulford, D. A.; Scheinberg, D. A.; Juricic, J. G. *J. Nucl. Med.* **2005**, *46* (Suppl 1), 199S.
- (125) (a) McDevitt, M. R.; Barendswaard, E.; Ma, D.; Lai, L.; Curcio, M. J.; Sgouros, G.; Ballangrud, A. M.; Yang, W.-H.; Finn, R. D.; Pellegrini, V.; Geerlings, M. W., Jr.; Lee, M.; Brechbiel, M. W.; Bander, N. H.; Cordon-Cardo, C.; Scheinberg, D. A. *Cancer Res.* **2000**, *60*, 6095. (b) Juricic, J. G.; Larson, S. M.; Sgouros, G.; McDevitt, M. R.; Finn, R. D.; Divgi, C. R.; Ballangrud, A. M.; Hamacher, K. A.; Ma, D.; Hamm, J. L.; Brechbiel, M. W.; Molinet, R.; Scheinberg, D. A. *Blood* **2002**, *100*, 1233.
- (126) Mulford, D. A.; Juricic, J. G. *Expert Opin. Biol. Ther.* **2004**, *4*, 95.
- (127) Couturier, O.; Supiot, S.; Degraef-Mougin, M.; Faivre-Chauvet, A.; Carlier, T.; Chatal, J.-F.; Davodeau, F.; Cherel, M. *Eur. J. Nucl. Med. Mol. Imaging* **2005**, *32*, 601.
- (128) Nikula, T. K.; McDevitt, M. R.; Finn, R. D.; Wu, C.; Kozak, R. W.; Garmestani, K.; Brechbiel, M. W.; Curcio, M. J.; Pippin, C. G.; Tiffany-Jones, L.; Geerlings, M. W., Sr.; Apostolidis, C.; Molinet, R.; Geerlings, M. W., Jr.; Gansow, O. A.; Scheinberg, D. A. *J. Nucl. Med.* **1999**, *40*, 166.
- (129) Qu, C. F.; Song, Y. J.; Rizvi, S. M. A.; Li, Y.; Smith, R.; Perkins, A. C.; Morgenstern, A.; Brechbiel, M.; Allen, B. *J. Cancer Biol. Ther.* **2005**, *4*, 848.
- (130) Kozak, R. W.; Atcher, R. W.; Gansow, O. A.; Friedman, A. M.; Hines, J. J.; Waldmann, T. A. *Proc. Natl. Acad. Sci. U.S.A.* **1986**, *83*, 474.
- (131) Ruegg, C. L.; Anderson-Berg, W. T.; Brechbiel, M. W.; Mirzadeh, S.; Gansow, O. A.; Strand, M. *Cancer Res.* **1990**, *50*, 4221.
- (132) Junghans, R. P.; Dobbs, D.; Brechbiel, M. W.; Mirzadeh, S.; Raubitschek, A. A.; Gansow, O. A.; Waldmann, T. A. *Cancer Res.* **1993**, *53*, 5683.
- (133) Simonson, R. B.; Ultee, M. E.; Hauler, J. A.; Alvarez, V. L. *Cancer Res.* **1990**, *50*, 985s.
- (134) Yao, Z.; Zhang, M.; Garmestani, K.; Axworthy, D. B.; Mallett, R. W.; Fritzberg, A. R.; Theodore, L. J.; Plascjak, P. S.; Eckelman, W. C.; Waldmann, T. A.; Pastan, I.; Paik, C. H.; Brechbiel, M. W.; Carrasquillo, J. A. *Clin. Cancer Res.* **2004**, *10*, 3137.

- (135) Norenberg, J. P.; Krenning, B. J.; Konings, I. R. H. M.; Kusewitt, D. F.; Nayak, T. K.; Anderson, T. L.; de Jong, M.; Garmestani, K.; Brechbiel, M. W.; Kvols, L. K. *Clin. Cancer Res.* **2006**, *12*, 897.
- (136) Nayak, T. K.; Norenberg, J. P.; Anderson, T. L.; Prossnitz, E. R.; Stabin, M. G.; Atcher, R. W. *Nucl. Med. Biol.* **2007**, *34*, 185.
- (137) Sofou, S.; Thomas, J. L.; Lin, H.-y.; McDevitt, M. R.; Scheinberg, D. A.; Sgouros, G. J. *Nucl. Med.* **2004**, *45*, 253.
- (138) (a) Twycross, R. G.; Fairfield, S. *Pain* **1982**, *14*, 303. (b) Hoskin, P. J.; Price, P.; Easton, D.; Regan, J.; Austin, D.; Palmer, S.; Yarnold, J. R. *Radiother. Oncol.* **1992**, *23*, 74. (c) Hoskin, P. J.; Ford, H. T.; Harmer, C. L. *Clin. Oncol. (R. Coll. Radiol.)* **1989**, *1*, 67.
- (139) Pecher, C. *Univ. Calif. Publ. Pharmacol.* **1942**, *2*, 117.
- (140) Srivastava, S. C. *Braz. Arch. Biol. Technol.* **2002**, *45*, 45.
- (141) Knapp, F. F., Jr.; Beets, A. L.; Mirzadeh, S.; Alexander, C. W.; Hobbs, R. L. *Czech. J. Phys.* **1999**, *49*, 799.
- (142) Mirzadeh, S.; Knapp, F. F., Jr.; Alexander, C. W.; Mausner, L. F. *Appl. Radiat. Isot.* **1997**, *48*, 441.
- (143) Maslov, O. D.; Starodub, G. Y.; Vostokin, G. K.; Gustova, M. V.; Dmitriev, S. N.; Shvets, V. N.; Szucs, Z.; Jansen, D.; Zeevaart, J. R. *Appl. Radiat. Isot.* **2011**, *69*, 965.
- (144) Lewington, V. J. *Phys. Med. Biol.* **1996**, *41*, 2027.
- (145) (a) Srivastava, S. C.; Meinken, G. E.; Richards, P.; Som, P.; Oster, Z. H.; Atkins, H. L.; Brill, A. B.; Knapp, F. F., Jr.; Butler, T. A. *Int. J. Nucl. Med. Biol.* **1985**, *12*, 167. (b) Oster, Z. H.; Som, P.; Srivastava, S. C.; Fairchild, R. G.; Meinken, G. E.; Tillman, D. Y.; Sacker, D. F.; Richards, P.; Atkins, H. L. *Int. J. Nucl. Med. Biol.* **1985**, *12*, 175. (c) Lewington, V. J. *J. Nucl. Med.* **2005**, *46*, 38S.
- (146) Atkins, H. L.; Mausner, L. F.; Srivastava, S. C.; Meinken, G. E.; Straub, R. F.; Cabahug, C. J.; Weber, D. A.; Wong, C. T.; Sacker, D. F.; Madajewicz, S. *Radiology* **1993**, *186*, 279.
- (147) Krishnamurthy, G. T.; Swailem, F. M.; Srivastava, S. C.; Atkins, H. L.; Simpson, L. J.; Walsh, T. K.; Ahmann, F. R.; Meinken, G. E.; Shah, J. H. *J. Nucl. Med.* **1997**, *38*, 230.
- (148) Deutsch, E.; Brodack, J. W.; Deutsch, K. F. *Eur. J. Nucl. Med.* **1993**, *20*, 1113.
- (149) Bruns, C.; Dietl, M. M.; Palacios, J. M.; Pless, J. *Biochem. J.* **1990**, *265*, 39.
- (150) Delpassand, E. S.; Sims-Mourtada, S.; Saso, H.; Azhdarinia, A.; Ashoori, F.; Torabi, F.; Espenan, G.; Moore, W. H.; Woltering, E.; Anthony, A. *Cancer Biother. Radiopharm.* **2008**, *23*.
- (151) (a) Cacheris, W. P.; Nickle, S. K.; Sherry, A. D. *Inorg. Chem.* **1987**, *26*, 958. (b) Kumar, K.; Chang, C. A.; Tweedle, M. F. *Inorg. Chem.* **1993**, *32*, 587. (c) Wadas, T. J.; Wong, E. H.; Weisman, G. R.; Anderson, C. J. *Chem. Rev.* **2010**, *110*, 2858. (d) Anderegg, G.; Nageli, P.; Muller, F.; Schwarzenbach, G. *Helv. Chim. Acta* **1959**, *42*, 827. (e) Clarke, E. T.; Martell, A. E. *Inorg. Chim. Acta* **1991**, *181*, 273. (f) Wu, S. L.; Horrocks, W. D., Jr. *J. Chem. Soc., Dalton Trans.* **1997**, 1497. (g) Martell, A. E.; Motekaitis, R. J.; Clarke, E. T.; Delgado, R.; Sun, Y.; Ma, R. *Supramol. Chem.* **1996**, *6*, 353. (h) Cotton, S. *Lanthanide and Actinide Chemistry*; John Wiley & Sons, Ltd: Chichester, England, 2006. Loncin, M. F.; Desreux, J. F.; Merciny, E. *Inorg. Chem.* **1986**, *25* (15), 2646–2648.